

AMERICAN UNIVERSITY OF BEIRUT

INVESTIGATING THE RESPONSE AND THE THERMAL
AXIAL FORCE DEMAND OF SHEAR TAB CONNECTIONS
WITH COMPOSITE BEAMS SUBJECTED TO FIRE
TEMPERATURES

by
MOHAMMAD ADIB HAJJAR

A thesis
submitted in partial fulfillment of the requirements
for the degree of Master of Engineering
to the Department of Civil and Environmental Engineering
of the Maroun Semaan Faculty of Engineering and Architecture
at the American University of Beirut

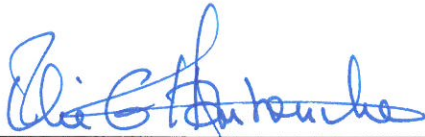
Beirut, Lebanon
November 2018

AMERICAN UNIVERSITY OF BEIRUT

INVESTIGATING THE RESPONSE AND THE THERMAL
AXIAL FORCE DEMAND OF SHEAR TAB CONNECTIONS
WITH COMPOSITE BEAMS SUBJECTED TO FIRE
TEMPERATURES

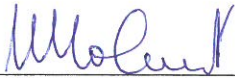
by
MOHAMMAD ADIB HAJJAR

Approved by:



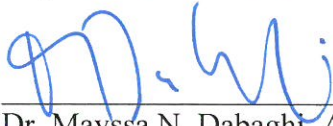
Dr. Elie G. Hantouche, Assistant Professor
Department of Civil and Environmental Engineering

Advisor



Dr. Mounir E. Mabsout, Professor
Department of Civil and Environmental Engineering

Member of Committee



Dr. Mayssa N. Dabaghi, Assistant Professor
Department of Civil and Environmental Engineering

Member of Committee

Date of thesis defense: November 26, 2018.

AMERICAN UNIVERSITY OF BEIRUT

THESIS, DISSERTATION, PROJECT RELEASE FORM

Student Name: Hajjar Mohammad Adile
Last First Middle

Master's Thesis Master's Project Doctoral Dissertation

I authorize the American University of Beirut to: (a) reproduce hard or electronic copies of my thesis, dissertation, or project; (b) include such copies in the archives and digital repositories of the University; and (c) make freely available such copies to third parties for research or educational purposes.

I authorize the American University of Beirut, to: (a) reproduce hard or electronic copies of it; (b) include such copies in the archives and digital repositories of the University; and (c) make freely available such copies to third parties for research or educational purposes after:

One --- year from the date of submission of my thesis, dissertation, or project.

Two ← years from the date of submission of my thesis, dissertation, or project.

Three --- years from the date of submission of my thesis, dissertation, or project.

[Signature]
Signature

December 18, 2018

Date

ACKNOWLEDGMENTS

First, I would like to acknowledge and thank my thesis advisor, Dr. Elie Hantouche, for his insistent support throughout my study. His expertise, dedication and enthusiasm were essential in the successful development of this research work. I appreciate his constant support and valuable critics which helped me develop my research skills, and knowledge throughout the time I spent at the American University of Beirut.

My recognition and gratitude are also extended to the thesis committee members, Dr. Mounir Mabsout and Dr. Mayssa Dabaghi. Their comments and encouragements were beneficial for the fulfilment of this research study.

I would like to acknowledge the financial support provided by the American University of Beirut Research Board under the grant No. 103604/project No. 24705.

Finally, I would like to express gratitude to my family, research team and friends for their support in the pursuit of my degree.

AN ABSTRACT OF THE THESIS OF

Mohammad Adib Hajjar for Master of Engineering
Major: Civil and Environmental Engineering

Title: Investigating the response and the thermal axial force demand of shear tab connections with composite beams subjected to fire temperatures

This study aims at developing a rational model to predict the thermal axial forces in shear tab connections with composite beams subjected to transient-state fire temperatures. Shear tab connections are one of the most commonly used simple beam-end framing connections. Simple connections are designed to resist shear forces at ambient temperature. During a fire event, large axial forces are generated due to the thermal expansion of the materials. These forces, which are not considered in the design, could lead to connection failure.

To achieve the aforementioned objective, finite element (FE) models are developed in ABAQUS and validated against experimental data available in the literature. Parametric FE simulations are then performed to investigate the effect of different parameters on the behavior of shear tab connections in composite beams during a fire. This includes: beam length, shear tab thickness, shear tab location, concrete slab thickness, setback distance, and degree of composite action. Based on the FE results obtained in this study, a design oriented model is developed to predict the thermal induced axial forces generated in the composite beams during the heating and cooling phases of a fire event. The proposed model consists of multi-linear springs that can predict the stiffness of each component of the connection and of the composite beam. The proposed model is capable of predicting the thermal axial forces in shear tab connections with composite beams under different geometrical properties.

The FE results show that the main factors that impact the behavior of shear tab connections with composite beams at elevated temperatures are: load ratio, setback distance, and bolt diameter. In addition, the creep in the concrete and the partial composite action result in larger displacements, however, they do not change the failure mode of the composite beam. Significant thermal axial forces are generated in the composite beam in fire as found in the FE results. This is prominent when the beam bottom flange comes in contact with the column. Fracture at the toe of the welds governs the behavior during the cooling phase in most FE simulations. The proposed rational model can predict the thermal axial force demand and can be used in performance-based approaches in future structural fire engineering applications.

CONTENTS

ACKNOWLEDGMENTS	V
ABSTRACT	VI
ILLUSTRATIONS	X
TABLES	XII
ABBREVIATIONS	XIII

Chapter

I. INTRODUCTION.....	1
II. FE MODELING OF SHEAR TAB CONNECTIONS WITH COMPOSITE BEAMS.....	7
A. Development of the FE model	7
1. Geometry of connection components.....	7
2. Boundary conditions	7
3. Loading conditions.....	8
4. Material properties	8
5. Model discretization.....	10
6. Analysis procedure/Heat transfer analysis	10
B. FE predictions vs. experimental results	11
III. EVALUATIONS OF DEMAND: PARAMETRIC STUDIES	15
A. Description of the composite beam model.....	15
B. Effect of key parameters and connection details.....	16
1. Beam length	16
2. Load ratio	17
3. Initial cooling temperature	18

4.	Shear tab location	18
5.	Shear tab thickness	19
6.	Slab thickness	19
7.	Setback distance	20
8.	Bolt diameter	21
9.	Effect of creep in the concrete	22
10.	Partial vs. full composite action	24
IV. RATIONAL MODEL DEVELOPMENT		41
A.	Description of the behavior	41
B.	Components Stiffnesses	42
1.	Shear tab and beam web in bearing.....	42
2.	Bolt in shear	43
3.	Axial stiffness of beam in contact with column.....	43
C.	Equivalent Connection Stiffness	43
D.	Thermal Axial Force	44
V. FORMULATION OF THE RESPONSE FOR THE PROPOSED MODEL		47
A.	Heating phase	47
1.	Stage 1 (s1).....	47
2.	Stage 2 (s2).....	47
3.	Stage 3 (s3).....	48
4.	Stage 4 (s4).....	49
B.	Cooling phase.....	50
5.	Stage 5 (s5).....	50
6.	Stage 6 (s6).....	50
7.	Stage 7 (s7).....	51
8.	Stage 8 (s8).....	51
VI. PROPOSED MODEL PERFORMANCE		54
VII. SUMMARY, CONCLUSIONS AND RECOMMENDATIONS		58
A.	Summary and Conclusions.....	58
B.	Recommendations	60

BIBLOGHRAPHY 62

ILLUSTRATIONS

Figure		Page
1.	FE assembly of the composite beam	12
2.	Strength retention factors K_{ut} for structural steel, structural bolts, shear stud, and weld material at elevated temperatures	12
3.	Experiment against. FE results (a) Deflection vs. Temperature and (b) Load-Deflection Response	13
4.	Shear tab connection during cooling (a) FE model and (b) Experiment (Selden et al. (2014))	14
5.	Layout of the connection assembly used in the parametric study	27
6.	Axial force and mid-span deflection for a varying beam length: (a) axial force and (b) mid-span deflection	28
7.	Axial force and mid-span deflection for a varying load ratio: (a) axial force and (b) mid-span deflection	29
8.	Axial force and mid-span deflection for a varying initial cooling temperature: (a) axial force and (b) mid-span deflection	30
9.	Axial force and mid-span deflection for a varying shear tab location: (a) axial force and (b) mid-span deflection	31
10.	Axial force and mid-span deflection for a varying shear tab thickness: (a) axial force and (b) mid-span deflection	32
11.	Axial force and mid-span deflection for a varying concrete slab thickness: (a) axial force and (b) mid-span deflection	33
12.	Axial force and mid-span deflection for a varying setback distance: (a) axial force and (b) mid-span deflection	34
13.	Axial force and mid-span deflection for a varying diameter of the bolts: (a) axial force and (b) mid-span deflection	35
14.	Shear force in the bolts along with the bolt strength for the two bolts diameter: (a) shear force for the 19 mm bolt and (b) shear force for the 25.4 mm bolt	36

15.	Axial force and mid-span deflection for both concrete defined as plastic and using CDP: (a) axial force and (b) mid-span deflection	37
16.	Axial force and mid-span deflection using implicit and explicit concrete models: (a) axial force and (b) mid-span deflection	38
17.	Axial force and mid-span deflection for composite beams with 19 mm diameter bolts: (a) axial force and (b) mid-span deflection	39
18.	Axial force and mid-span deflection for composite beams with 25 mm diameter bolts: (a) axial force and (b) mid-span deflection	40
19.	Typical variation of the axial force in the composite beam with temperature	46
20.	Components incorporated in the assembly of the equivalent connection stiffness	46
21.	Ratio of the yielded area of the beam web to the total web area (A_{by}/A_{bw}) against temperature	52
22.	Summary of different stages present in the proposed model	52
23.	Proposed model vs. FE results (a) Case 1, (b) Case 2, (c) Case 3, (d) Case 4, (e) Case 5, (f) Case 6	55
24.	Proposed model vs. FE results (a) Case 7, (b) Case 8, (c) Case 9, (d) Case 10	56

TABLES

Table		Page
1.	Parametric study cases in FE modeling	54

ABBREVIATIONS

E	elastic modulus of steel material
f_y and F_y	yield strength of steel
f_u , and F_u	ultimate strength of steel
F_{EXX}	electrode strength of weld
f'_c	ambient compressive strength of concrete
w	uniform load
$f_c(T)$	compressive strength of the concrete at temperature T
ϵ_{exp}	explicit concrete strain
ϵ_{cl}	concrete strain at peak stress
σ	concrete stress
K_{br}	shear/beam web stiffness in bearing
n_b	number of bolt rows
k_b and k_t	factors related to the section properties as defined in Eurocode 3
d	diameter of the bolt
K_{bolt}	bolt stiffness in shear
d_{M16}	nominal diameter of an M16 bolt type
K_c	contact stiffness
A_{bf}	area of the area of the lower flange of the beam

L	span length of the beam
$E_{avg.}$	average modulus of elasticity of steel
K_e	equivalent connection stiffness
$K_{bolt-row}$	total stiffness of all the components at each bolt
P	thermal axial force
Δ	displacement
E_s	modulus of elasticity of the steel beam
A_{bw}	beam web area
α	coefficient of thermal expansion
ΔT	temperature increment
A_t	transformed concrete area
A_c	area of the concrete slab
E_c	modulus of elasticity of concrete
P_{cr}	critical buckling force
ϵ_e	elastic strain limit
ϵ_c	strain in the concrete
ΔT_s	temperature increment in the steel beam
ΔT_c	temperature increment in the concrete slab
P_y	yielding force
E_T	tangent modulus

A_{by}	yielded area of the beam web
a and b	constants used to obtain the yielded area of the beam web
$E_{avg.}$	average elastic modulus of steel
θ_c	rotation at which contact occurs
s	setback distance
h	steel beam height
θ	beam end rotation
I	moment of inertia

CHAPTER I

INTRODUCTION

A composite beam is a structural element composed of a steel beam and a concrete slab joined together to act as one unit. The compressive strength of concrete combined with the tensile strength of steel at ambient temperature, give the composite system the required strength and ductility. Composite action between steel and concrete is established through the use of shear studs which are welded to the top flange of the steel beam. Different types of steel connections are used to connect the steel beam to the column. Shear tab connections are simple steel connections that are widely used in steel buildings, and they play a crucial role in maintaining the stability of steel structures under gravity loading. According to current design guidelines, these connections are considered as pinned connections and are designed to resist vertical shear forces at ambient temperature. However, during a fire event, the connection behavior is more complex due to thermal induced forces and deformations generated in the beam end connections. During the heating phase, these forces are first compressive due to axial restraint against thermal expansion before turning into tensile forces at the post fire-cooling stage. The large thermal induced forces and deformations accompanied with strength and stiffness degradation of the connection components can lead to connection failure and consequently to structural collapse.

Many studies were conducted in the past few years to investigate the behavior of shear tab connections with composite beams under fire. For instance, Wald et al. (2006) studied the behavior of a steel-concrete composite floor with shear tab connections under fire. The results show that buckling occurred at the beam bottom flange and shear tab

failure occurred due to the large axial forces generated in the connection. In addition, Garlock & Selamet (2010) performed analytical studies to assess the behavior of shear tab connections with composite beams at elevated temperatures. Linear springs were attached to the top flange of the beam to account for flexural stiffness of the concrete slab. The connection endured the heating phase and failed in the cooling phase due to the large axial tensile forces generated in the beam. Furthermore, Agarwal et al. (2014) studied the failure modes of composite floor systems in a ten-story steel building subjected to fire. Excessive deflections occurred in the composite beam accompanied with large rotations at its ends. Then as the beam bottom flange came in contact with the column flange, large axial forces were generated in the beam leading to connection failure. Selden et al. (2014, 2016) performed full scale experiments on shear tab connections with composite beams subjected to fire loading. Shear tab fracture at the toe of the weld occurred during the cooling phase of the fire. Also, Choe et al. (2018) conducted experimental tests on composite beams with double angle connections subjected to fire temperatures. The results showed that failure was initiated at the interface between the shear studs and the concrete and the test was terminated when fracture of the welds occurred.

Moreover, Pakala & Kodur (2016) conducted experimental and numerical studies to investigate the effect of the concrete slab on the behavior of subframe assemblies with double angle connections exposed to fire. Two assemblies were analyzed, one with the concrete slab and the second without the concrete slab. The presence of the concrete slab enhanced the rigidity of the connection and it prevented local and lateral torsional buckling of the steel beam by providing a lateral restraint. Three-dimensional (3D) FE models were performed by Fischer & Varma (2015, 2017) to study the behavior of composite beams with simple connections subjected to gravity loads and different fire

scenarios. The parameters varied included the duration of the fire, the fire resistance rating of the beam, the deck type and the connection type. It was found out that bolt shear fracture was the controlling limit state for composite beams with simple connections along with a flat concrete slab, while fracture of the shear tab was observed in beams with a metal deck. Additional numerical studies were performed by Selden & Varma (2016) to model the behavior of composite beams under fire. The results showed that the material model available in Eurocode 4 (2005) can be used to model the response of composite beams at elevated temperatures, but it provides conservative predictions for the composite beams deflections for temperatures above 500 °C. However, using the material model proposed by Phan et al. (2010) underestimates the deflections for temperatures above 500 °C. Selamet & Bolukbas (2016) carried out a numerical investigation on the performance of a composite floor system with shear tab connections at elevated temperatures. It was shown that the connection experiences severe deflections and rotations exceeding its capacity causing bolts failure.

Creep in the concrete is considered a long-term time dependent behavior. Tarantino & Dezi (1992) developed a numerical model for the viscoelastic analysis of composite beams at ambient temperature, and then a numerical analysis was performed to study the effect of the main parameters on the response. It was found that the creep stresses generated in the concrete slab are gradually transferred to the top flange of the steel beam, which causes an increase in the deflection. At elevated temperatures, thermal creep occurs in concrete due to rupture of the bonds in the microstructure of the cement paste. Gernay & Franssen (2012) developed a mathematical formulation for the explicit strain in concrete (excluding the creep strain). They assumed that the creep strain depends on the stress and the temperature and not on the time. Another important factor which

affects the behavior of composite beams is the percentage of composite action in the beam. This factor was studied in part 1 by Wang et al. (2016) as experimental studies were conducted accompanied by numerical studies in part 2 by Wang et al. (2016). It was concluded that the partial composite action induces larger interface slip between the steel beam and the concrete slab and higher deflection when compared to full composite action at high temperatures (above 500 °C). The aforementioned experimental and numerical studies indicate that shear tab connections with composite beams cannot withstand the thermal induced axial forces during the fire event. This highlights the need for more research on evaluating the induced thermal axial forces and including them in design procedures to ensure safe predictions.

Recently, there have been studies on performance-based fire engineering and is expected that structural fire engineering design approach to be adopted and implemented by the industry in coming years. For instance, in the US, the final report on the world trade center towers collapse (NIST NCSTAR, (2005)) recommended the use of performance-based methods as an alternative to current methods in the fire resistance design of structures. Furthermore, Appendix E of ASCE (2017) now permits designers to use structural fire engineering as an alternative to prescriptive approaches. Besides, Appendix 4 of AISC (2016) recommends developing advanced design methods that explicitly account for the deterioration in strength and stiffness, the effects of thermal expansion, time effects, and potential limit states. Alternatively, rational models can be developed using multi-linear springs that are combined together to predict thermal axial force and deformation demands at elevated temperatures.

Rational models were developed to predict the thermal response of other types of connections in bare steel beams, such as flush endplate (Jones (1997) and El Ghor &

Hantouche (2017)), shear endplate (Hu et al. (2009) and Hantouche & Sleiman (2017)), double angle (Hantouche et al. (2018)) and top and seat angle connections (El Kalash & Hantouche (2017)). For instance, Hu et al. (2009) proposed a rational model for shear end plate connections to predict the force-rotation behavior of the connection at elevated temperatures. Also, Hantouche & Sleiman (2017) developed a rational model to predict the axial restraint forces in steel frames with shear endplate connections during a fire. In addition, many studies were conducted to develop rational models for predicting the behavior of shear tab connections. Koduru & Driver (2014) proposed a rational model for the force-rotation of isolated shear tab connections at elevated temperatures. Besides, Sarraj (2007) developed a rational model for predicting the thermal forces in shear tab connections with bare steel beams. However, very limited research work was conducted to develop a rational model for composite connections at ambient and elevated temperature. For instance, Jones (1997) studied the performance of bare and composite flush endplate connections subjected to fire temperatures. Rational models for the corresponding connections were developed in accordance with the experimental studies conducted. Also, Piluso et al. (2012) developed a rational model for composite connections under hogging and sagging moments. The shear studs and the concrete slab are incorporated in the model, however, only the response at ambient temperature was considered. All these studies did not develop a rational model capable of predicting the induced axial force developed in shear tab connections with composite beams when subjected to fire.

To address these shortcomings, in this research, the behavior of shear tab connection with composite beam under fire is investigated, by developing FE models and a rational model for design. First, FE models are developed and validated against

experimental studies performed by Selden et al. (2014). A heat transfer analysis is performed to predict the temperature distribution in the composite beam. Second, FE models are developed to conduct a parametric study to identify the major parameters that affect the behavior of shear tab connections with composite beams under fire. This includes the geometrical components of the connection, in addition to the creep effect in the concrete as per the proposed model by Gernay & Franssen (2012). Also, the effect of composite action (full vs. partial) on the performance of shear tab connections with composite beams in fire is investigated. Finally, the results of the FE analysis are used to assemble a rational model to predict the thermal axial forces developed in shear tab connections with composite beams when exposed to fire temperatures.

CHAPTER II

FE MODELING OF SHEAR TAB CONNECTIONS WITH COMPOSITE BEAMS

This section describes the development of the FE model in ABAQUS. Results from the FE model of shear tab connection with composite beam are compared with those obtained from the experimental study conducted by Selden et al. (2014, 2016). It is noted that the purpose is not only to reproduce the experimental results using FE modeling, but also to conduct FE simulations on the parameters that impact the behavior of shear tab connections with composite beams in fire.

A. Development of the FE model

1. Geometry of connection components

The composite beam consists of a W10×22 steel beam with a lightweight concrete slab. The slab has a thickness of 89 mm (3.5 in.) and an effective width of 914 mm (36 in.). Composite action between steel and concrete is established using shear studs of diameter 12.7 mm spaced at 152 mm, yielding a partial composite action of 37%. The composite beam is connected to the W14×109 column with a single shear tab connection (6.35 mm x 114 mm x 152 mm) that is welded to a thick plate which is connected to the column. The weld is 6.35 mm thick and 152 mm long. The shear tab is connected to the beam using two 19 mm (3/4 in.) diameter A325 bolts. An overall view of the model is shown in Fig. 1.

2. Boundary conditions

Boundary conditions are applied throughout the analysis as shown in Fig. 1. First, pretensioning of the bolts is applied. Then, a vertical load of 156 kN (35 kips) is applied monotonically at the mid-span of the beam. This load is held constant while applying heating to the desired temperature, followed by the cooling step. During the pretensioning step, the bolts are restrained against any translation to ensure contact between the bolt head and nut, and the base material. Also, the top and bottom ends of the column are fixed against translation and rotation. In the loading step, the boundary conditions applied in the pretension step are deactivated except the restraint on the top and bottom of the column. The composite beam is restrained against lateral displacement to avoid lateral torsional buckling throughout the analysis.

3. Loading conditions

Transient temperature analysis is performed to study the performance of the shear tab connection with composite beam in fire. Before the heating step, the composite beam is loaded in two sequential steps. In the first step, pretension force is applied to all bolts. In the second step, a vertical load of 156 kN (35 kips) is applied monotonically at the mid-span of the beam. This load is held constant throughout the heating phase. During the cooling phase, the load is kept constant until reaching a bottom flange temperature of 250 °C, at which the applied load is decreased by 30%. After the specimen cooled to 150 °C, the applied load is completely removed.

4. Material properties

Steel material

An idealized bilinear model is used for the steel material. The mechanical properties for the steel beam and column at ambient temperature are: the yield stress $F_y = 394$ MPa (57.1 ksi) and the ultimate stress $F_u = 541$ MPa (78.6 ksi), which are in accordance with the experimental data performed by Selden et al. (2016). The yield and

ultimate stresses used for the shear tab connection are $F_y = 317$ MPa (46 ksi) and $F_u = 448$ MPa (65 ksi), respectively. For the A325 bolts used, the ultimate stress $F_u = 930$ MPa (135 ksi) is included in the model. Also, the weld with electrode strength $F_{EXX} = 756$ MPa (110 ksi) is included in the model. The shear studs are modeled with yield stress $F_y = 350$ MPa (51 ksi) and ultimate stress $F_u = 450$ MPa (65 ksi), respectively, according to the structural welding code (American Welding Society AWS, (2010)). To represent the behavior of all materials at elevated temperatures, retention factors are used to estimate the mechanical properties of material (including the elastic modulus, E). For the base material, retention factors proposed by Hu et al. (2009) are used, while for the bolts and the weld the retention factors used are obtained from AISC (2010) specifications and Eurocode 3 (2005), respectively. The model proposed by Zhao & Kruppa (1997) is used to represent the strength degradation of the shear studs at high temperatures. Fig. 2 shows the retention factors for the mechanical properties of the steel material, shear studs, bolts, and weld used in the FE model.

Concrete material

The concrete compressive strength at ambient temperature used in the model is $f'_c = 54.4$ MPa (7.7 ksi) as per Selden et al. (2016). Concrete damage plasticity (CDP) is used to model the concrete behavior. The CDP model, developed by Lee & Fenves (1998), uses the concept of isotropic damaged elasticity in combination with isotropic tensile and compressive plasticity to represent the inelastic behavior of concrete. The failure of concrete is assumed to be governed by two failure modes: (1) concrete crushing in compression, or (2) concrete cracking in tension. The stress-strain relationships

available in Eurocode 4 (2005) are used to model the concrete behavior under compression and tension at elevated temperatures.

5. Model discretization

Eight-node brick elements with reduced integration (C3D8-R) are used to mesh the different components present in the ABAQUS model. The mesh configuration is shown in Fig. 1. To increase the accuracy of the results, a finer mesh is used at the connection region where high stresses develop and failure is likely to occur. In addition, the segment of the beam near the point load application is subject to a refined mesh, as well as the areas surrounding the shear studs. A mapped meshing technique is used to discretize bolts and the adjacent areas to account for stress concentration around the bolt holes.

Surface to surface contact with a finite sliding coefficient is used to reproduce contact surfaces between the bolt shank, shear tab, and the steel beam. A friction coefficient of 0.3 is used to allow for separation, sliding, and rotation of the contact surfaces. A sacrificial plate is placed between the column and the beam to protect the column from the fire temperatures. Tie constraint is used to connect the weld to each of the shear tab and the sacrificial plate. For the connection between the shear studs and the slab, a constraint is created to model the studs as the embedded region and the concrete slab as the host region. The shear studs are connected to the top flange of the beam using a tie constraint. Also, a tie constraint is defined to model the interaction between the column flange and the sacrificial plate.

6. Analysis procedure/Heat transfer analysis

Transient analysis is conducted to predict the response of the shear tab connection with composite beam subjected to thermal loading, including both heating and cooling

phases of a fire. The temperature distribution along the depth of the beam is obtained from heat transfer analysis. In the heat transfer analysis, the temperature at specified locations in the beam is set equal to the values recorded in the experiment conducted by Selden et al. (2014), then the temperature in all locations is derived from the heat flux generated in the beam. The maximum temperature reached in the model occurs at the bottom flange and is equal to 600 °C. The temperature dependent thermal conductivity values for concrete and steel available in Eurocode 2 (2004) and Eurocode 3 (2005), respectively, are used. The output from the heat transfer model is extracted and applied as a thermal load on the composite beam in the stress analysis model.

B. FE predictions vs. experimental results

The FE results of the shear tab connection with composite beam are compared to the experimental data available in the literature (Selden et al. 2014). Figs. 3(a) and 3(b) show the deflection as a function of temperature and the load-deflection response, respectively, for the experiment and the FE predictions. It can be seen from Figs. 3(a) and 3(b) that the FE model predicts with reasonable accuracy the deflection-temperature and load-deflection responses, respectively.

Fig. 4 shows a comparison of the actual deformed shape of the shear tab connection during the cooling phase of the experiment against the FE results. It can be seen that the failure of the shear tab occurs at the toe of the weld. Therefore, the FE model is capable of predicting the failure mode of the connection, as shown in Fig. 4.

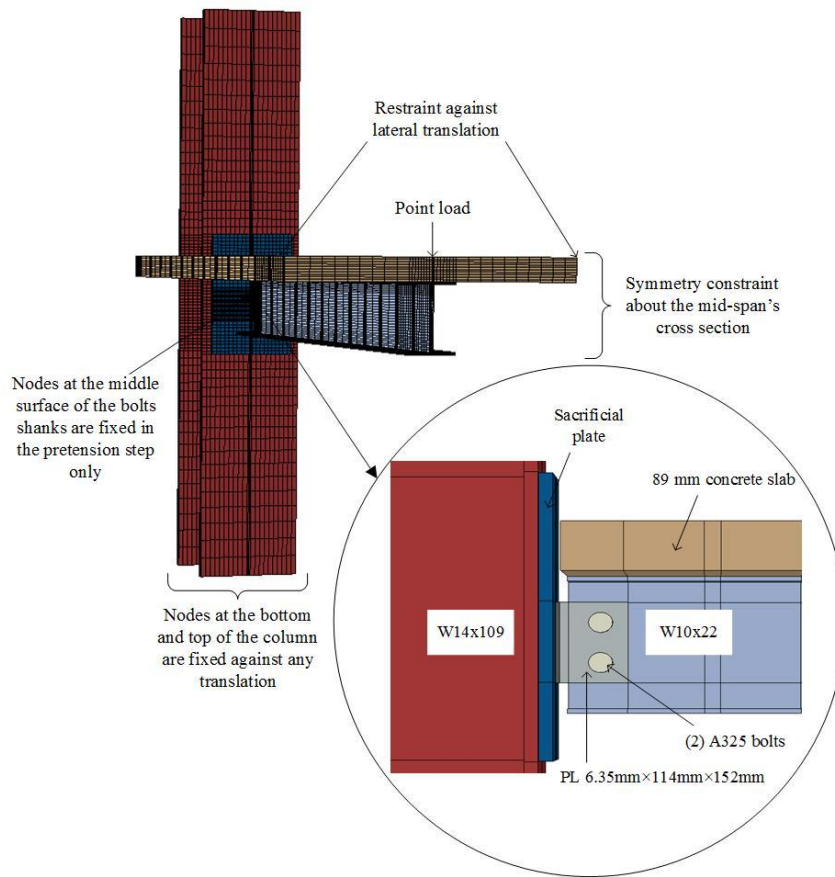


Figure. 1. FE assembly of the composite beam

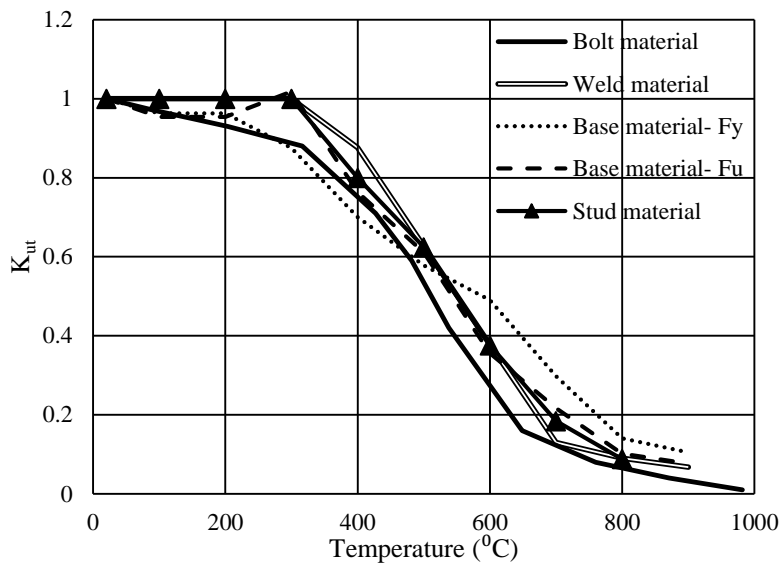
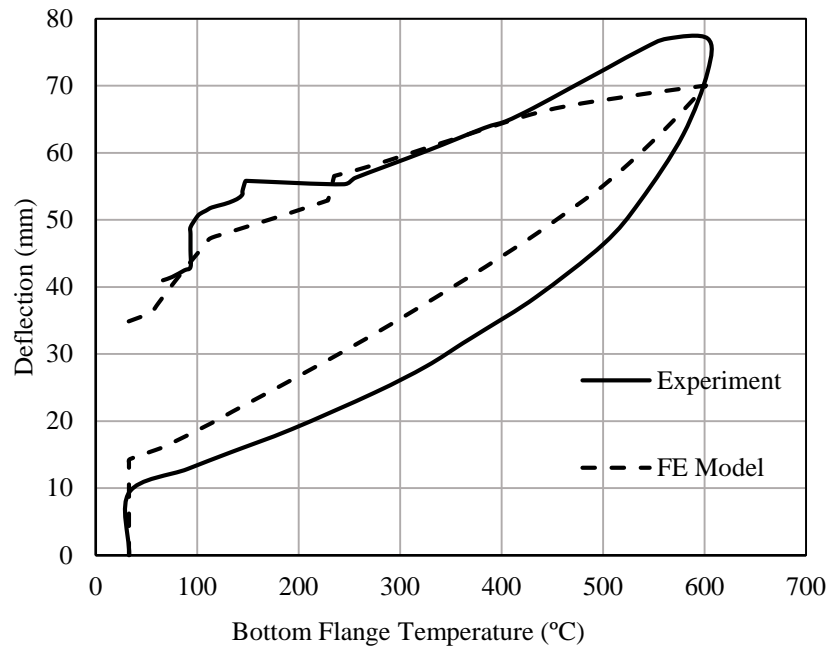
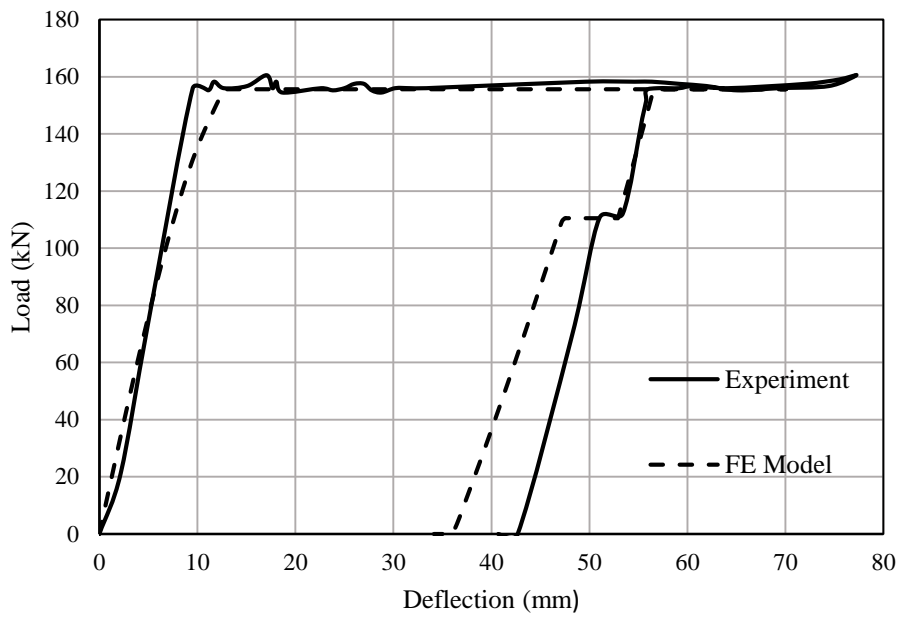


Figure. 2. Strength retention factors K_{ut} for structural steel, structural bolts, shear stud, and weld material at elevated temperatures

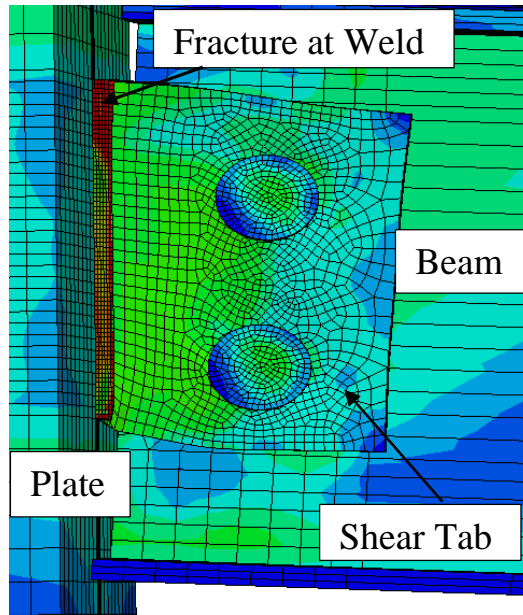


(a)

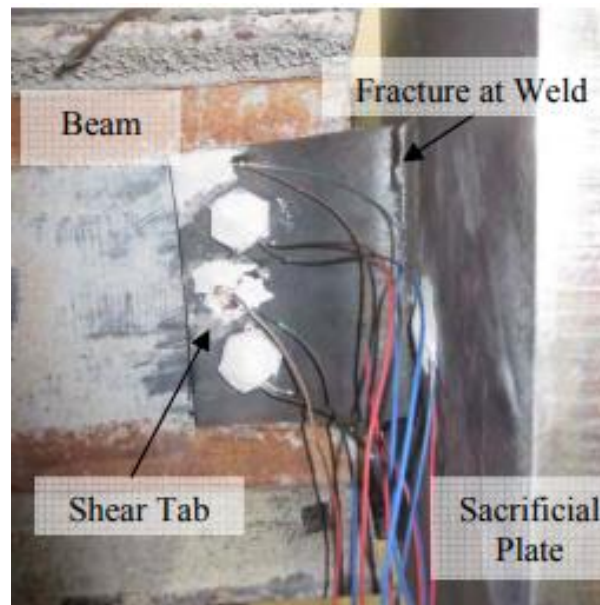


(b)

Figure. 3. Experiment against. FE results (a) Deflection vs. Temperature and (b) Load-Deflection Response



(a)



(b)

Figure. 4. Shear tab connection during cooling (a) FE model and (b) Experiment (Selden et al. (2014))

CHAPTER III

EVALUATIONS OF DEMAND: PARAMETRIC STUDIES

This section presents the key parameters that impact the behavior of shear tab connections in composite beams at elevated temperatures. FE models are developed in ABAQUS and used to conduct a series of parametric studies on the behavior of shear tab connections with composite beams in fire. The fire is idealized into a *temperature-time* history curve which varies from 20 °C to 650 °C, then drops back to 20 °C to represent the cooling phase.

A. Description of the composite beam model

In this parametric study, the beam used is a W16×36, spanning between two W14×90 columns. The concrete slab thickness is 91 mm. The beam ends are attached to the columns using shear tab connections bolted to the beam web and welded to the column flange, as shown in Fig. 5. The bolt diameter is 25.4 mm (1 in.) and the setback is 20.3 mm (0.8 in.). The material properties for the bolts, weld and base material at ambient temperature are the same as the ones used in the FE model described in the previous section done to reproduce the experiment performed by Selden et al. (2014). The concrete compressive strength at ambient temperature is assumed to be 35 MPa (4.95 ksi). The column segment used is 3.05 m long and assumed pinned at its top and bottom ends. A uniformly distributed load is applied to the beam. The magnitude of the uniform load varies to produce a maximum moment equal to a certain ratio of the plastic moment capacity of the composite beam at ambient temperature.

The top and bottom faces of the column are braced against translation and rotation in all directions during the analysis. Also, the composite beam is braced against lateral displacement along its length. Transient analysis is performed, as the temperature increases from 20 °C up to the desired temperature, and then drops back to 20 °C while keeping the applied load. The bottom flange of the beam reaches an ultimate temperature of 650 °C, while the web and the connection are heated up to 400 °C. Only part of the column which is aligned with the connection as shown in Fig. 5 is heated, while the remaining part is assumed to be isolated to prevent thermal expansion of the column and consequently generating additional axial forces in the column. The slab is heated up to a temperature of 300 °C, except otherwise modified as per the parametric study. The choice of the magnitude of the temperature and its distribution is a good idealization of a real fire. The composite beam modeled is assumed to have full composite action between the concrete slab and the steel beam. Thus, a tie constraint is created to connect the concrete slab with the steel beam's top flange.

B. Effect of key parameters and connection details

The parameters examined are: beam length, load ratio, initial cooling temperature, shear tab location, shear tab thickness, slab thickness, setback distance, bolt diameter, concrete creep effect, and degree of composite action.

1. Beam length

The effect of the beam length on the connection behavior is studied. Beams having a length of 6.10 m (20 ft.), 9.15 m (30 ft.), and 12.20 m (40 ft.) are selected. The load ratio used for all beams is 0.5. Figures 6(a) and 6(b) show the variation of the axial force in the beam and the mid-span deflection with respect to the connection temperature, respectively. The results show that only 6.10 m long beam survived the heating phase,

however, it failed during the cooling phase at a connection temperature of 145 °C. In this case, and during the cooling phase, tensile forces developed in the beam. Then, the applied load gradually changes from flexural to tensile until the tensile axial force exceeds the tensile capacity of weld leading to fracture at the toe of the weld. The beams with spans of 9.15 m and 12.20 m both failed at the toe of the weld in the heating phase at a temperature of 330 °C and 290 °C, respectively. As it can be seen from Fig. 6 that the axial force increases rapidly at the early stages of heating phase until beam web buckling occurs around a connection temperature of 150 °C. After this temperature, the axial force continues to increase but at a slower rate. For the 12.20 m beam span, the flexural stiffness is lower than the other beams causing contact to occur earlier at a connection temperature of 200 °C, as shown in Figs. 6(a) and 6(b). For the 9.15 m beam length, contact occurs at a later stage of the heating phase (at a temperature of 270 °C) leading to an increase in the axial force. This analysis shows that increasing the beam length results in larger deflection and larger compressive axial force that causes failure (fracture at the toe of weld) to occur earlier.

2. Load ratio

The load ratio is defined as the ratio of the maximum moment generated in the beam due to the applied uniform load to the nominal plastic moment capacity of the composite beam cross section, M_p , at ambient temperature. The moment developed in the beam at its mid-span is assumed to be equal to $wl^2/8$, where w is the uniform load applied and l is the span length. The span length of the beam is 6.1 m (20 ft.), which is considered a typical span for beams used in composite construction. The load ratios used in the analysis are 0.25, 0.50 and 1.00.

Figures 7(a) and 7(b) show the axial force and the mid-span deflection as a function of temperature, respectively, for the three load ratios. It is observed from Fig. 7(a) that increasing the load ratio from 0.25 to 0.5 does not produce a significant change in the axial force, as fracture of the weld occurred during the cooling phase in the two beams. Also, it can be seen from Fig. 7(b) that the beam with a load ratio of 1.0 develops the largest deflection. This initiates contact between the beam and the column at a connection temperature of 325 °C. Consequently, the axial force increases rapidly until failure occurs at a temperature of 375 °C. In conclusion, increasing the load ratio to 1.0 causes failure of the weld to occur earlier.

3. Initial cooling temperature

To study the effect of the initial cooling temperature on the response of shear tab connection with composite beam, a 6.10 m long beam with a load ratio of 0.5 is modeled. Three values of the initial cooling temperature are considered: 400 °C, 500 °C and 650 °C, only the bottom flange temperature is changed. The variation of the axial force and the deflection with respect to the connection temperature are shown in Figs. 8(a) and 8(b), respectively. It can be seen from Fig. 8(a) that the beam with 650 °C initial cooling temperature develops the largest tensile axial force through the cooling phase. The three beams survived the heating phase and failed during the cooling phase at a connection temperature of 145 °C. Increasing the initial cooling temperature produces larger deflections at mid-span due to the additional loss of stiffness at higher temperatures (see Fig. 8(b)). When the initial cooling temperature is 650 °C, contact between the beam and the column occurs right before the end of the heating, but it did not produce a significant effect on the maximum axial compressive force.

4. Shear tab location

Another parameter incorporated in this study is the location of the shear tab on the connection behavior in fire. Two locations for the shear tab are selected for this analysis; the first location is at mid height of the steel beam and the second one at 20 mm above the center of the steel beam. The FE results show that in both cases the shear tab connection with composite beam failed at the toe of the weld in the cooling phase. Figures 9(a) and 9(b) illustrate the axial force and the mid-span deflection with respect to the connection temperature, respectively. The results show that the response of the composite beam did not change when the shear tab is shifted upward. In this case the eccentricity (20 mm) is not large since the shear tab covers a large part of the beam web, and as a result no significant impact on the behavior was noticed.

5. Shear tab thickness

Two values for the shear tab thicknesses are used: 9.5 mm (0.375 in.) and 12.7 mm (0.5 in.). Figures 10(a) and 10(b) represent the axial force developed in the composite beam with respect to the connection temperature for both cases. It can be seen from Fig. 10(b) that for a shear tab thickness of 12.7 mm the compressive axial force is slightly larger than that of 9.5 mm shear tab thickness. The two beams survived the heating phase and failed during the cooling phase at the toe of a weld at a connection temperature equal to 145 °C. This indicates that thicker shear tab results in a more stiff connection that leads to generate more axial forces during the heating phase.

6. Slab thickness

To study the effect of the thickness of the concrete slab, three cases are considered: (1) 66 mm (2.6 in.), (2) 91 mm (3.6 in.), (3) 114 mm (4.5 in.). For the 66 mm thick slab, the plastic neutral axis (PNA) is located in the top flange of the steel beam, while in other cases (91 mm and 114 mm) the PNA is located in the concrete slab. Figures 11(a) and

11(b) show the axial force and the deflection as a function of the connection temperature, respectively, for the three cases. As shown in Fig. 11(a), the axial force is approximately the same in the three beams until the contact occurs in the beam with 66 mm thick slab at a temperature of 370 °C. As a result, the axial force reached in this beam is the largest among the three cases. The connection survived the heating phase and failed at the toe of the weld in the cooling phase, in the three cases. It can be seen from Fig. 11(b) that the beam with the 66 mm slab experiences the largest deflection. Hence, increasing the concrete slab thickness affects the deflection response of the composite beam, and consequently it affects the axial force due to the contact which occurs between the beam's bottom flange and the column.

7. *Setback distance*

The setback is assumed to be equal to the distance between the edge of the beam flange and the column flange (see Fig. 5). The setback is controlled by the following three factors: (1) shear tab width, (2) edge distance of the beam web, and (3) the distance between the bolt line and the weld line of the shear tab. To study the influence of the setback distance on the behavior of the shear tab connection, three values of the setback are considered: (1) 12.7 mm (0.5 in.), (2) 20.3 mm (0.8 in.), and (3) 25.4 mm (1 in.).

For a setback of 12.7 mm, contact occurs between the beam flange and the column flange at a connection temperature of 270 °C, as shown in Fig. 12(a). This contact causes the axial force to increase leading to fracture of the shear tab at the toe of the weld. For the 20.3 mm setback, contact still occurs between the beam and the column but at a higher temperature (385 °C). When the setback distance is 25.4 mm, no contact occurs and consequently the maximum axial force in the connection is lower than other cases. It can be seen from Fig. 12(b) that the deflection is the same in the three cases until the contact

occurs for the beam with 12.7 mm setback. The beams with setback values of 20.3 mm (0.8 in.) and 25.4 mm (1 in.) survived heating and failed during cooling at a connection temperature of 145 °C. Thus, a small setback distance causes an earlier contact between the beam bottom flange and column that results in larger compressive forces developed in the beam end connection.

8. Bolt diameter

The effect of the diameter of the shear bolts is examined by using two different bolt diameters: 19 mm (3/4 in.) and 25.4 mm (1 in.). The span of the beam considered is 6.10 m and the load ratio is 0.5. Figures 13(a) and 13(b) show the axial force and the deflection as a function of temperature, respectively, for each bolt diameter. It can be seen from Fig. 13(a) that when the bolt diameter is 25.4 mm (1 in.), the axial compressive force is larger than that when the bolt diameter is 19 mm (3/4 in.). During the cooling phase, the tensile force is larger for the case when the bolt diameter is 19 mm (3/4 in.). This force causes failure of the weld to occur at a temperature of 240 °C. The beam with a bolt diameter of 25.4 mm (1 in.) survived heating and failed during cooling. The deflection in the beam with 19 mm (3/4 in.) bolt diameter is larger than the case where 25.4 mm (1 in.) bolts are used, as shown in Fig. 13(b). Contact occurs between the beam's bottom flange and the column flange at a temperature of 320 °C for the beam with 19 mm (3/4 in.) bolts diameter. While for the beam with 25.4 mm (1 in.) bolts, contact occurs just before the end of the heating phase.

The variation of the shear force in the lower bolt of the connection with respect to the bolt temperature is shown in Figs. 14(a) and 14(b) for the 19 mm (3/4 in.) and 25.4 mm (1 in.) diameter bolts, respectively. The estimated bolt shear strength as a function of temperature is also shown in each figure. The shear strength of the bolt is calculated

according to the AISC specifications (2016). Figure 14(a) shows that for the 19 mm (3/4 in.) bolt, the maximum shear force of 110 kN is reached at a temperature of 200 °C. For the 25.4 mm (1 in.), the maximum shear force of 160 kN is reached a temperature of 300 °C, as shown in Fig. 14(b). It can be seen that no shear failure is predicted in the bolts for the two values of the bolt diameter. It can be concluded that increasing the bolt diameter results in lower deflections and larger axial compressive forces.

9. *Effect of creep in the concrete*

Thermal creep strain develops in the concrete when subjected to compression at elevated temperatures. Creep is implicitly included in the stress-strain relationship of concrete available in Eurocode 4 (2005). However, the drawback of the implicit model is that the creep strain is irreversible. That is, when a concrete specimen is cooled down, the creep strain is recovered, which does not reflect the true behavior. For this purpose, Gernay & Franssen (2012) developed a stress-strain relationship for concrete, where the total strain term does not include the creep strain. The model proposed by Gernay & Franssen (2012) is shown below:

$$\frac{\sigma}{f_c(T)} = \frac{2\varepsilon_{\text{exp}}}{\varepsilon_{c1} \left[1 + \left(\frac{\varepsilon_{\text{exp}}}{\varepsilon_{c1}} \right)^2 \right]} \quad (1)$$

where $f_c(T)$ is the compressive strength of the concrete at temperature T , ε_{exp} denotes the explicit strain (excluding the creep strain), ε_{c1} is the strain corresponding to peak stress, and σ is the stress in the concrete. ε_{c1} is a function of the peak stress strain values available in Eurocode 2 (1995, 2004). The creep strain is then obtained by subtracting the explicit strain proposed by Gernay & Franssen (2012) from the implicit strain available in Eurocode 4 (2005).

In order to model the creep in the concrete, a user subroutine that includes the creep strain is developed and included in the ABAQUS model. The limitation of including a creep subroutine in ABAQUS is that the CDP could not be used to model the concrete material. As a result, the concrete is modeled as plastic and analyzed by assuming it has the same strength in tension and in compression. Consequently, having tension in the concrete does not provide accurate results. Therefore, the composite beam studied is designed so that the PNA is located in the steel beam, and all the concrete section is in compression. To evaluate the accuracy of assuming the concrete as plastic, the results obtained when modeling the concrete as plastic are compared to those obtained when modeling the concrete using CDP, excluding the creep effect in concrete. The composite beam is heated up to 550 °C with a uniform distribution over the cross section. The axial force and the deflection versus temperature for both models are shown in Figs. 15(a) and 15(b), respectively. It can be concluded that there is no significant difference in the axial force and the deflection. Thus, it is acceptable to model the concrete material as plastic.

To study the effect of creep in the concrete on the behavior of composite beams under fire, a comparison between implicit and explicit concrete models is performed. The implicit model uses the stress strain relationship available in Eurocode 4 (2004), where the creep strain is implicitly included as a part of the total concrete strain. The explicit model uses the formulation proposed by Gernay & Franssen (2012) which presents a relationship between the stress and the explicit strain (see Eq. (1)). In this case, the subroutine that includes the creep strain is implemented in the ABAQUS model. The modulus of elasticity used in the model is the one proposed by Gernay & Franssen (2012). The span length of the beam is 6.10 m, the slab thickness is 63 mm (2.5 in.) and the steel beam used is a W16 x 36. The temperature distribution is uniform all over the cross

section and it is equal to 550 °C. It can be seen from Fig. 16(a) that there is no significant difference in the axial force between the results of the two models. This is due to the fact that the axial force developed in the steel beam is much larger than that developed in the concrete slab since the thermal expansion of the steel is larger than that of the concrete (Eurocode 2 (2004), Eurocode 3 (2005)). Also, contact between the beam bottom flange and the column occurs around a temperature of 515 °C. Fracture of the weld is observed in both models at a temperature of 450 °C during the cooling phase. Fig. 16(b) shows that the deflection increases as the temperature increases until reaching a temperature of 515 °C. Then, the deflection decreases during the cooling phase. The decrease in deflection in the cooling phase is larger for the implicit model. This is because in the implicit model the creep strain is recovered during the unloading (cooling) step. While in the explicit model, only the elastic strain is recovered since the creep strain is irreversible. This leads to larger permanent deflections in the explicit model. The results agree with the findings of Gernay & Franssen (2012) as there is a significant difference between implicit and explicit concrete models in the cooling phase. It is found from this analysis that the concrete creep increases the deflection of the composite beam.

10. Partial vs. full composite action

To study the effect of the partial composite action, a beam with 38% composite action is modeled in ABAQUS and compared with one having full composite action. The full composite beam is modeled using a tie constraint between the concrete slab and the steel beam's top flange. For the partial composite beam, shear studs of 19 mm (3/4 in.) diameter are used at a spacing of 381 mm (15 in.). The shear studs are modeled as embedded in the concrete slab, and they are connected to the top flange of the beam using a tie constraint. The beam is W16 x 36 with a 91 mm (3.6 in.) thick concrete slab. The

beam span is 6.10 m and the load ratio is 0.5. The diameter of the bolt used in the connection is 19 mm (3/4 in.). The axial force and the mid-span deflection versus temperature are shown in Figs. 17(a) and 17(b), respectively. The maximum axial force in the partial composite beam is slightly greater than that with full composite action, as shown in Fig. 17(a). It can be seen from Fig. 17(b) that the deflection in the partial composite beam is larger than the deflection in the full composite beam. This is due to the fact that the flexural stiffness of the full composite beam is larger than that of the partial composite beam. Contact between the beam and the column occurs at a temperature of 345 °C and 355 °C for the partial and full composite beams, respectively. Moreover, the failure mode (fracture of the weld) is the same in the two beams. Thus, the partial composite action does not produce a significant impact on the behavior of the composite beam.

The same analysis is repeated with the diameter of the bolt used is 25.4 mm (1 in.) instead of 19 mm (3/4 in.). Full and partial composite beams are modeled with the same properties stated in the previous paragraph. Figs. 18(a) and 18(b) show the axial force and the mid-span deflection as a function of temperature, respectively. It can be seen from Fig. 18(a) that there is not a significant difference in the axial force for the full and partial composite beams. Contact between the beam and the column occurs after reaching a temperature of 370 °C. So the contact did not have a significant impact on the axial force. Also, the deflection of the partial composite beam is larger than that of the full composite one, as shown in Fig. 18(b). Both beams survived heating and failed during cooling around a temperature of 145 °C. In conclusion, the partial composite beam encounters larger displacement at elevated temperatures. However, the axial force and the failure mode are the same for beams with full and partial composite action. That is, the behavior

of the partial composite beam is similar to that of the full composite one. This conclusion agrees with the experimental studies performed in part 1 by Wang et al. (2016), where experimental tests were performed on partial and full composite beams.

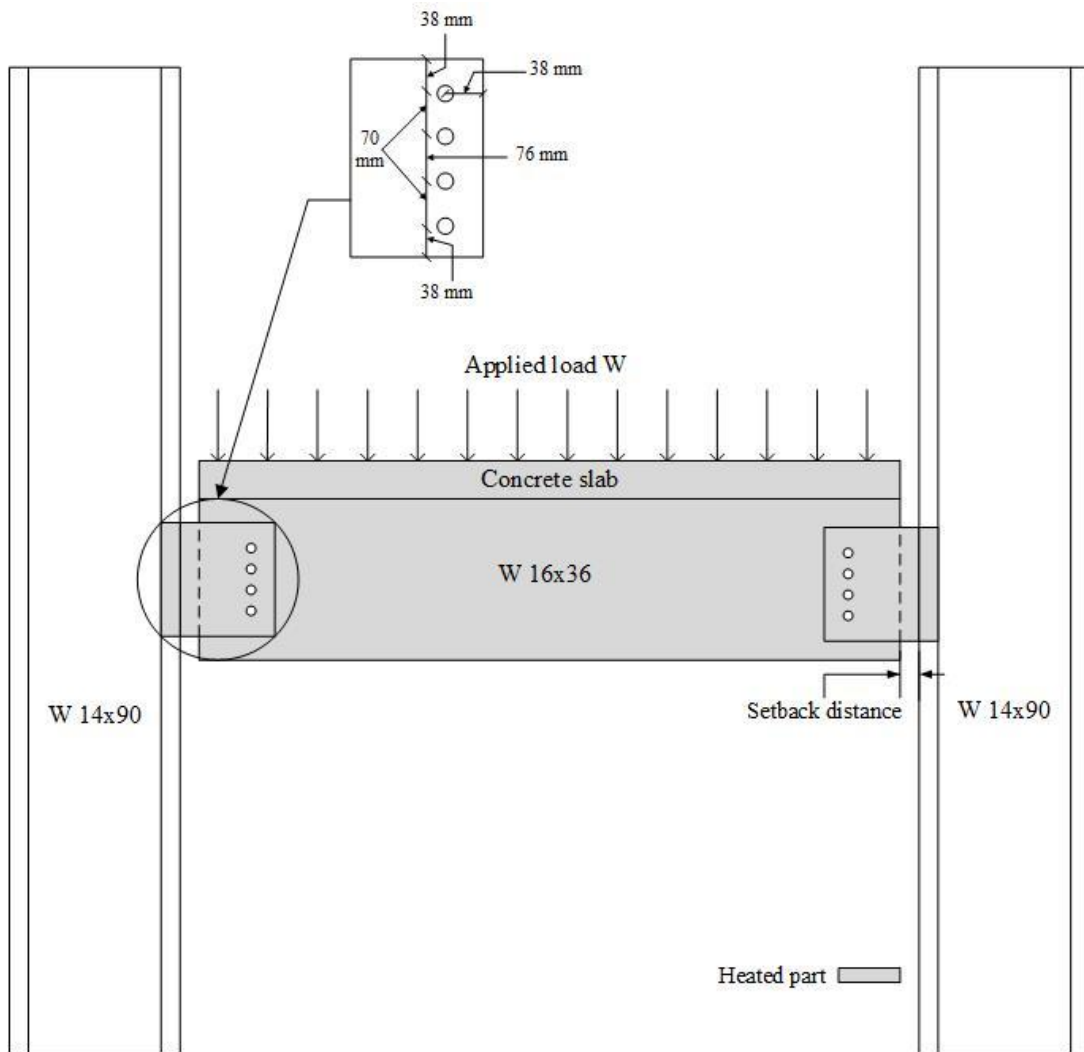
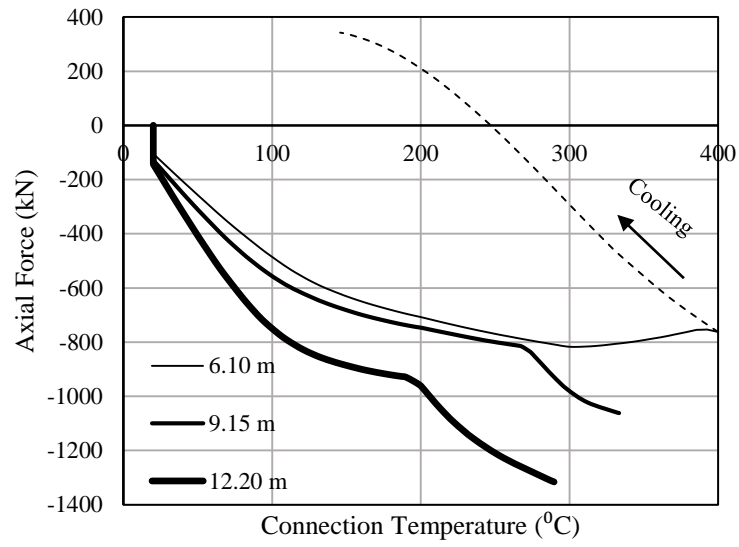
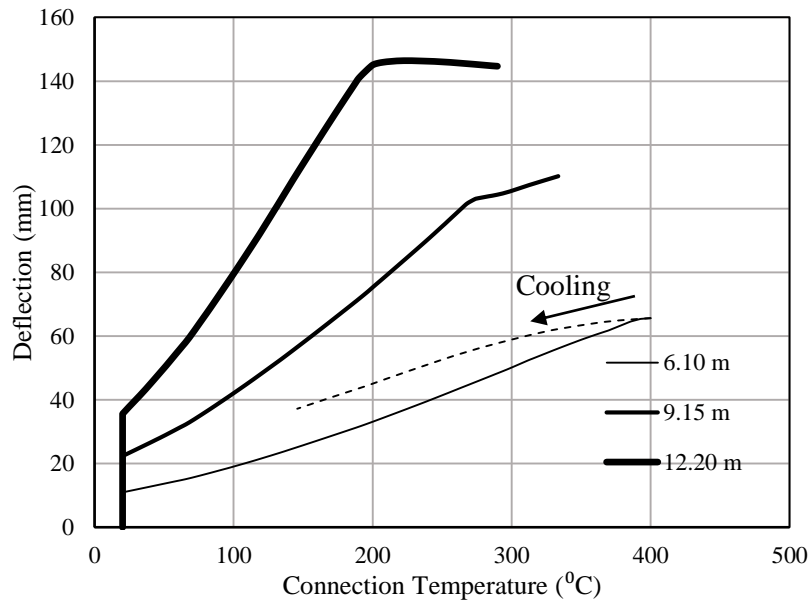


Figure. 5. Layout of the connection assembly used in the parametric study

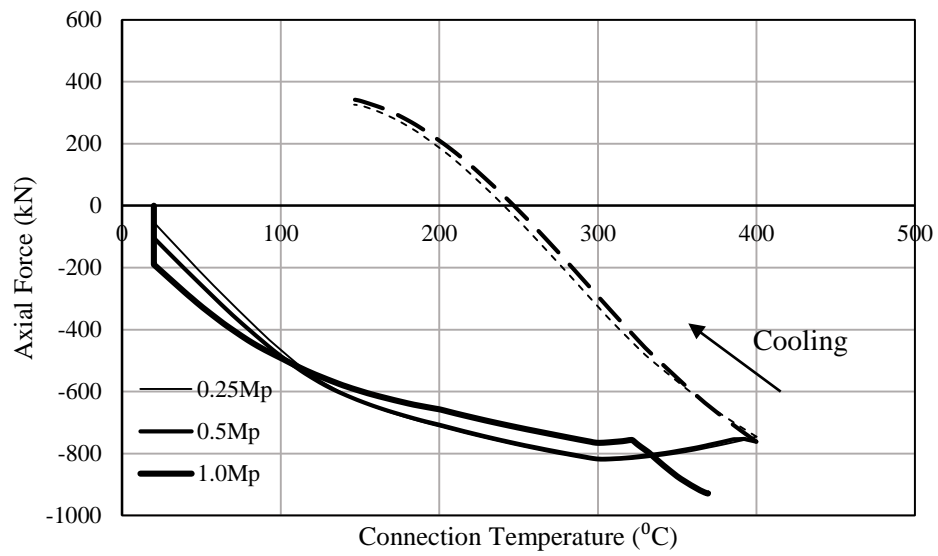


(a)

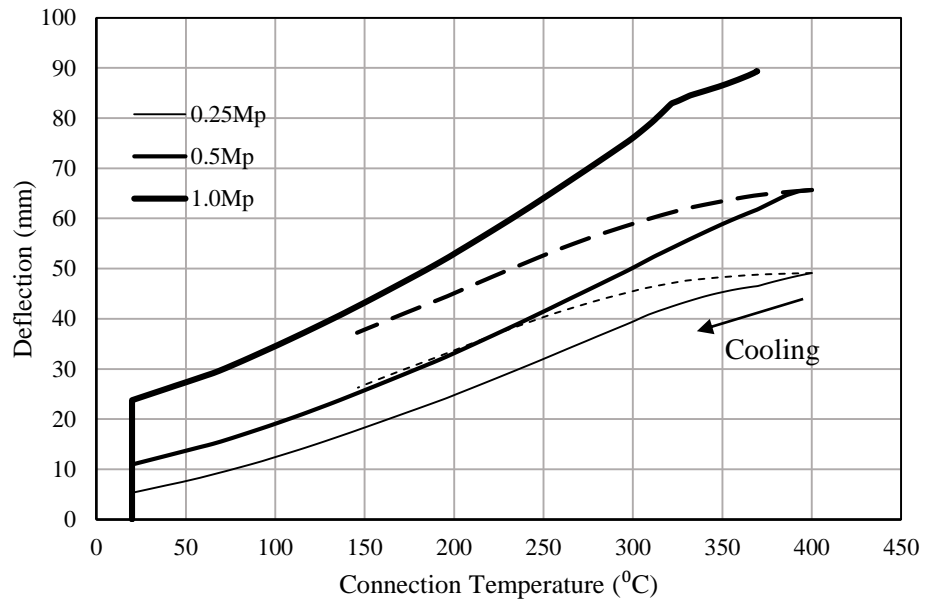


(b)

Figure. 6. Axial force and mid-span deflection for a varying beam length: (a) axial force and (b) mid-span deflection

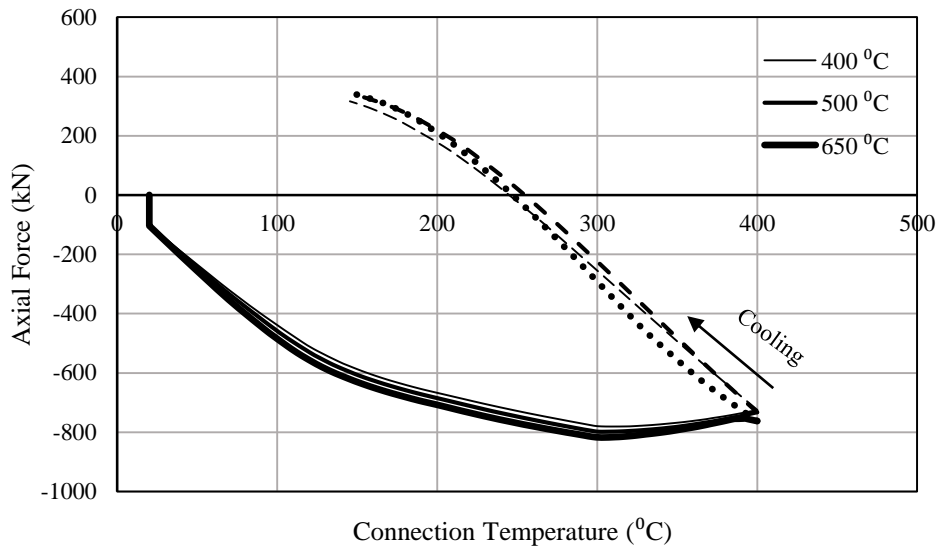


(a)

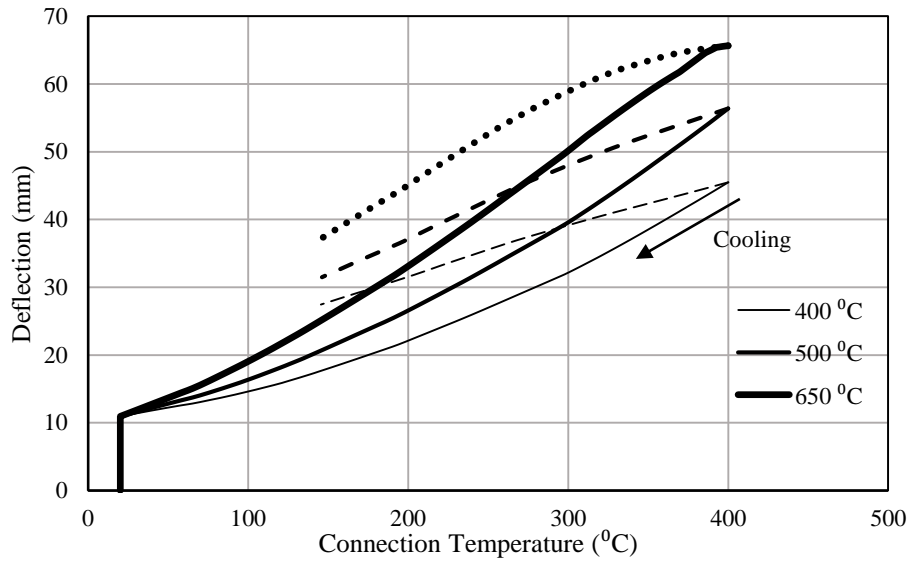


(b)

Figure. 7. Axial force and mid-span deflection for a varying load ratio: (a) axial force and (b) mid-span deflection

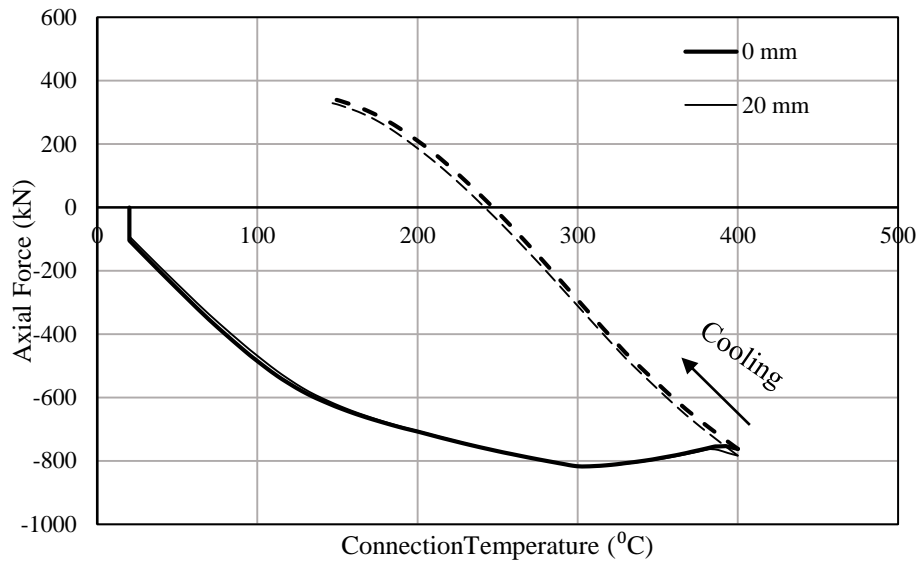


(a)

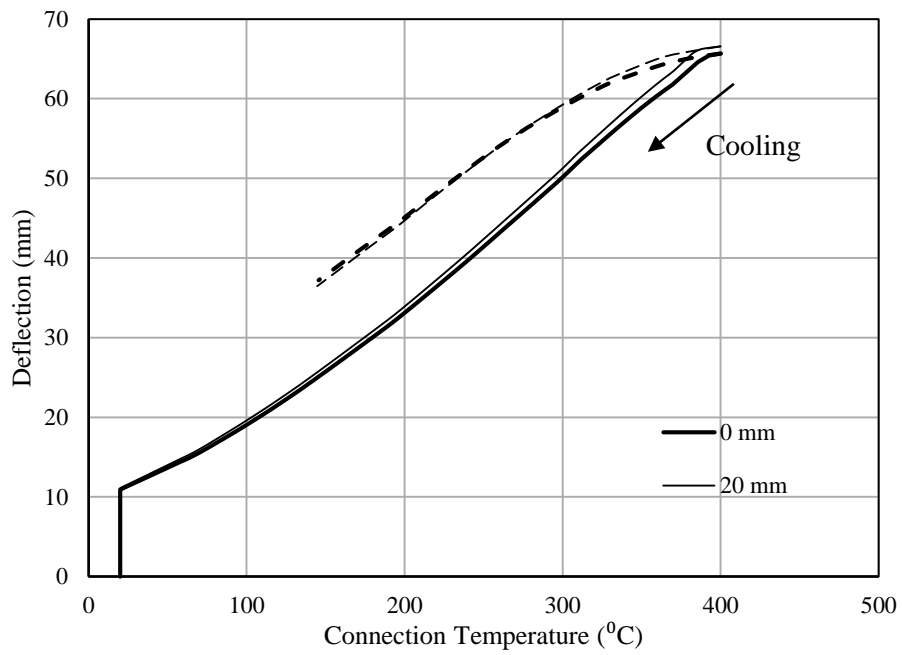


(b)

Figure 8. Axial force and mid-span deflection for a varying initial cooling temperature: (a) axial force and (b) mid-span deflection

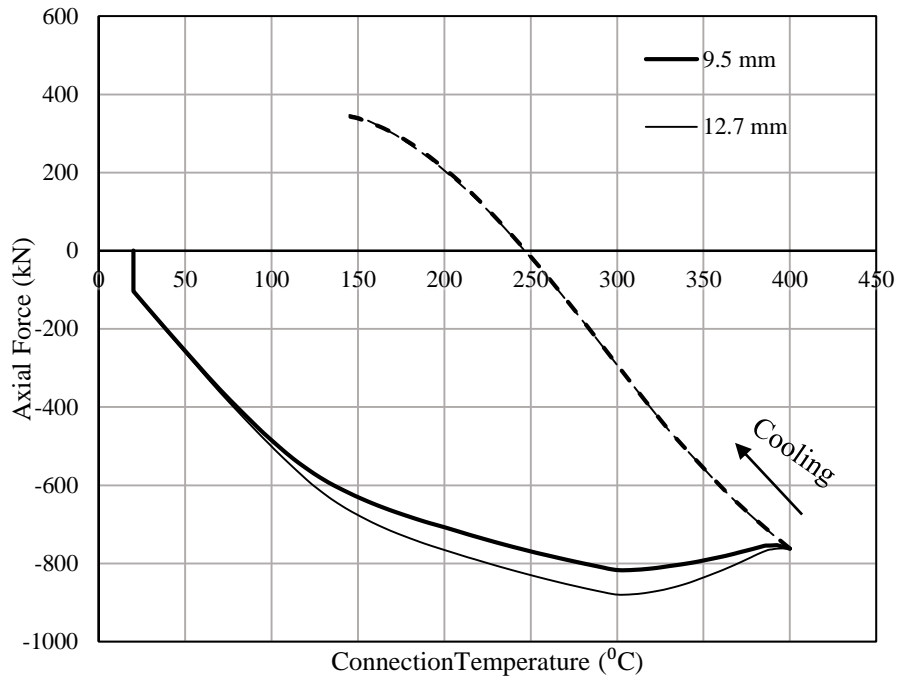


(a)

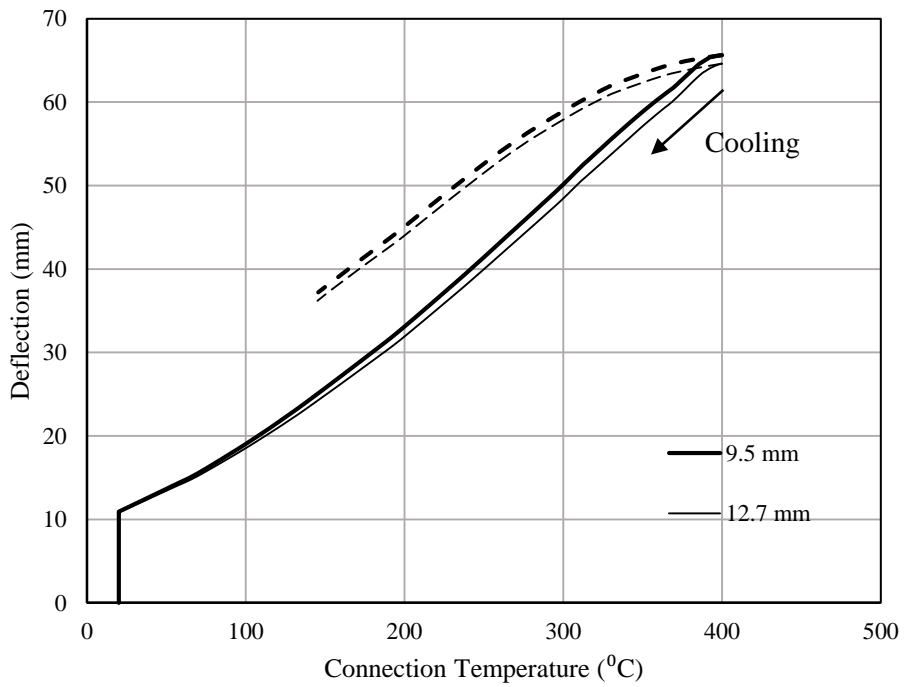


(b)

Figure. 9. Axial force and mid-span deflection for a varying shear tab location: (a) axial force and (b) mid-span deflection

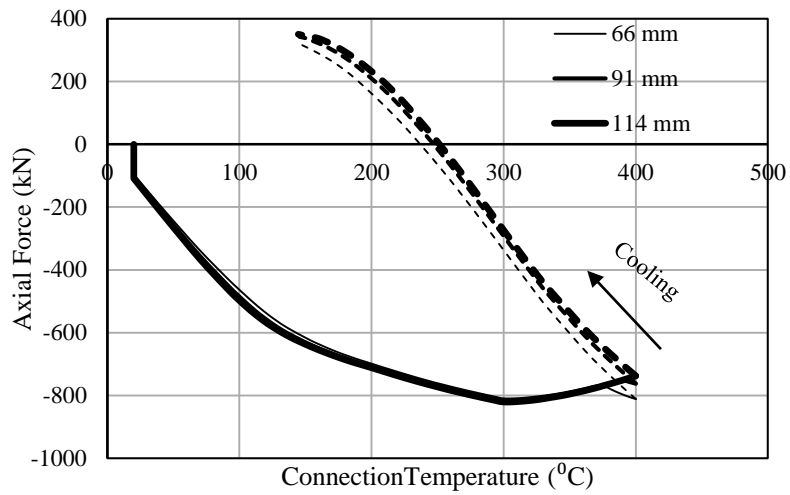


(a)

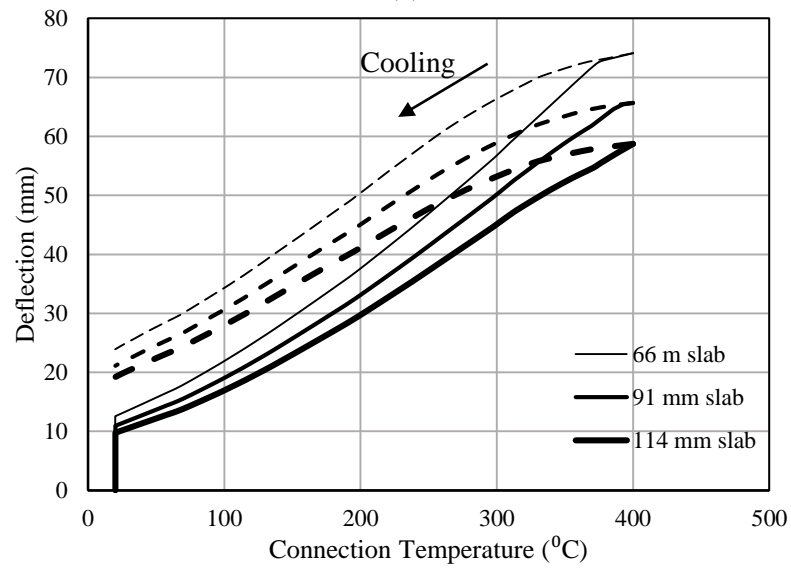


(b)

Figure. 10. Axial force and mid-span deflection for a varying shear tab thickness: (a) axial force and (b) mid-span deflection

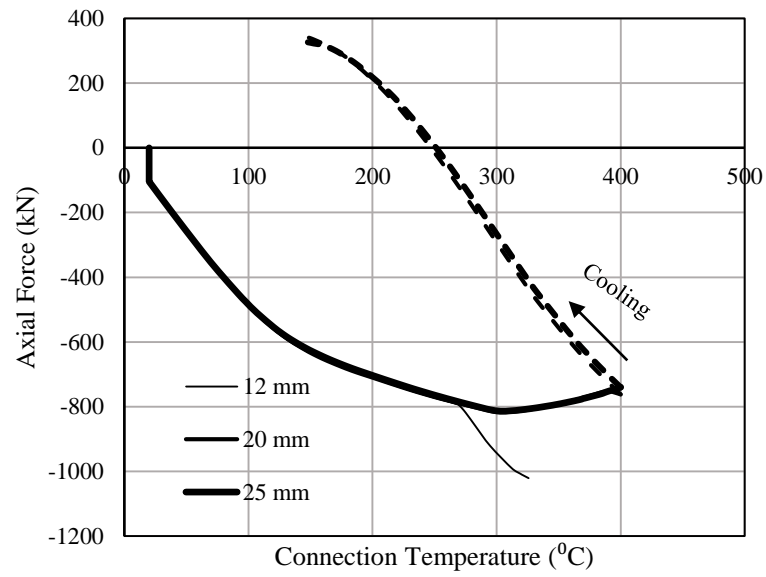


(a)

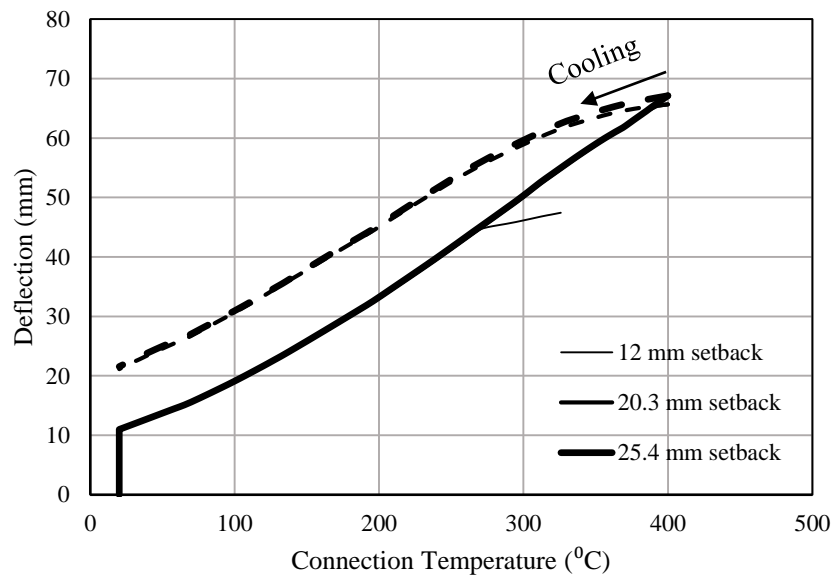


(b)

Figure. 11. Axial force and mid-span deflection for a varying concrete slab thickness:
 (a) axial force and (b) mid-span deflection

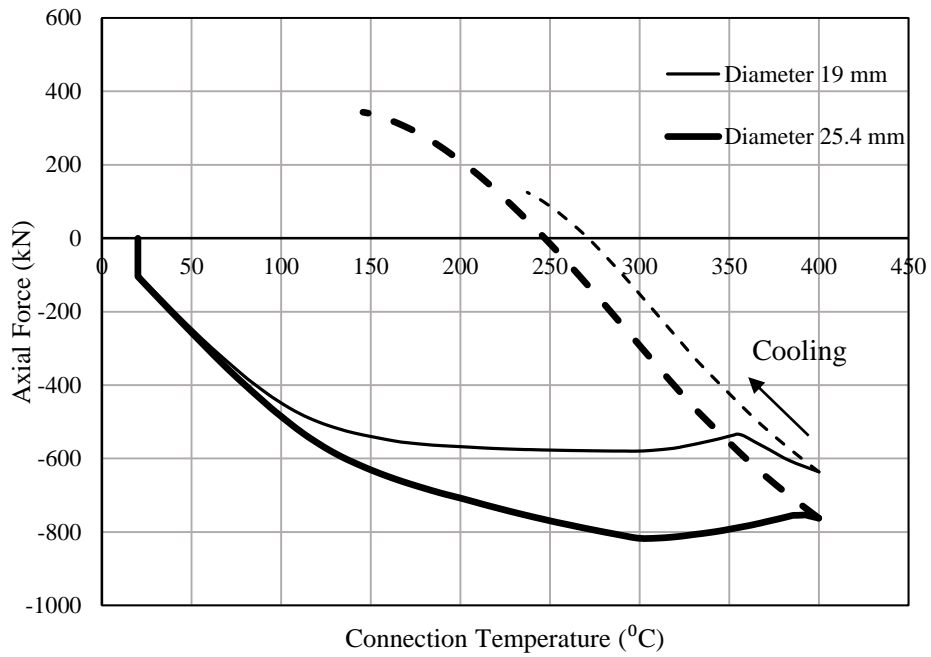


(a)

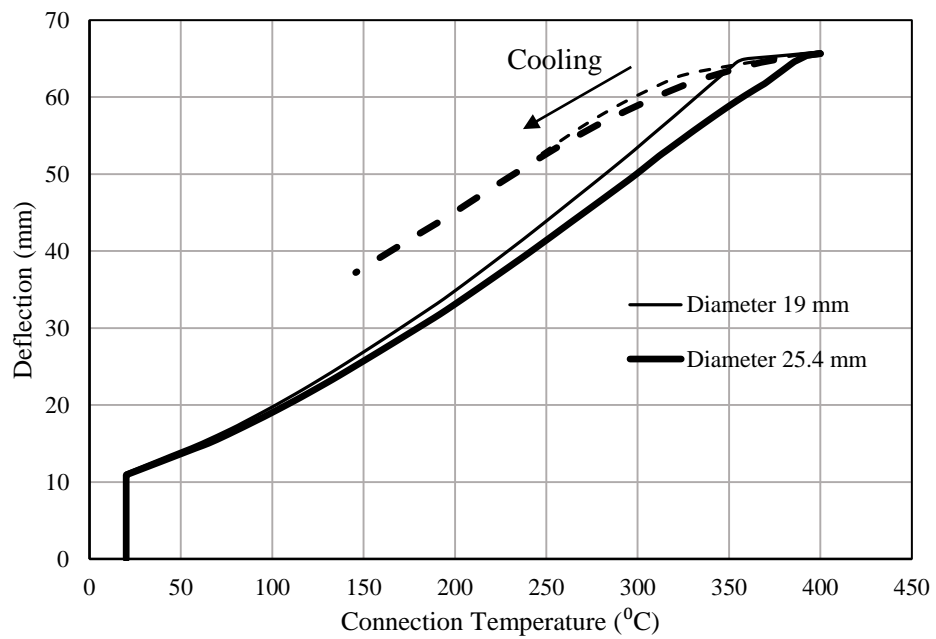


(b)

Figure. 12. Axial force and mid-span deflection for a varying setback distance: (a) axial force and (b) mid-span deflection

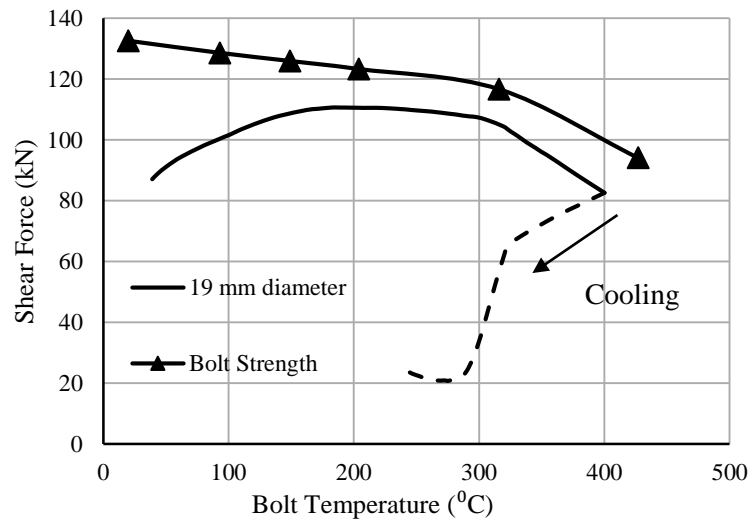


(a)

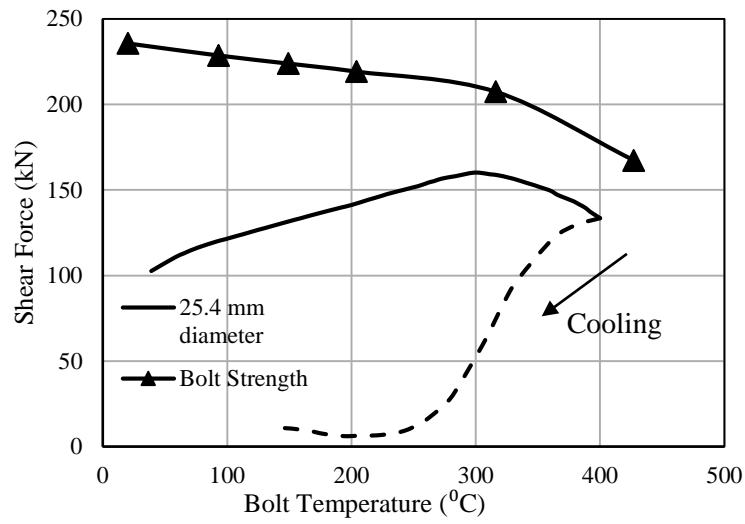


(b)

Figure. 13. Axial force and mid-span deflection for a varying diameter of the bolts: (a) axial force and (b) mid-span deflection

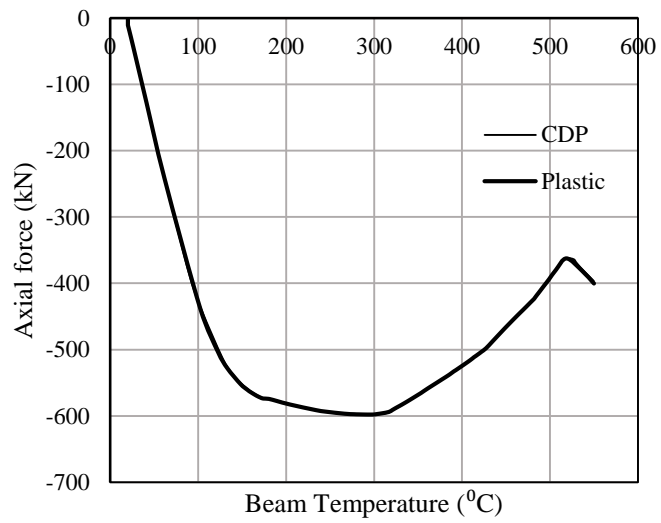


(a)

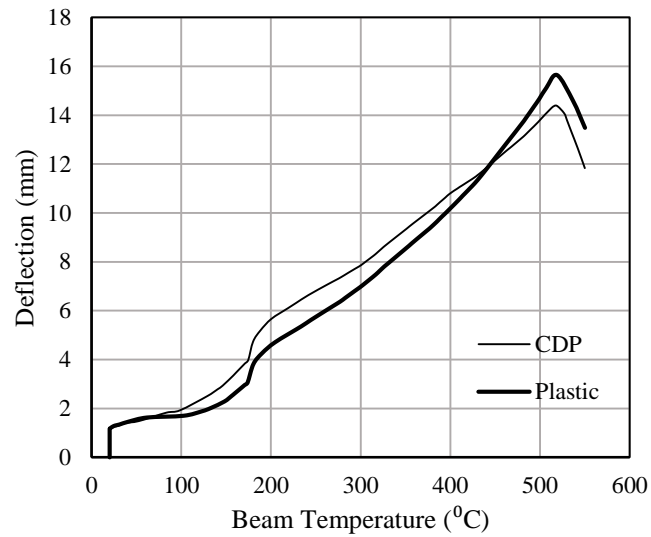


(b)

Figure. 14. Shear force in the bolts along with the bolt strength for the two bolts diameter: (a) shear force for the 19 mm bolt and (b) shear force for the 25.4 mm bolt

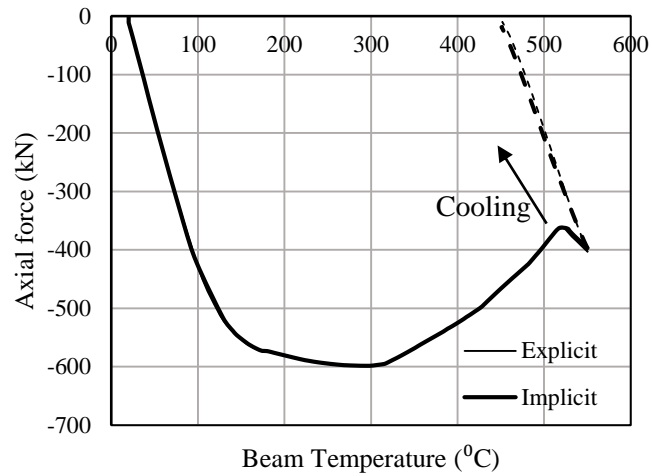


(a)

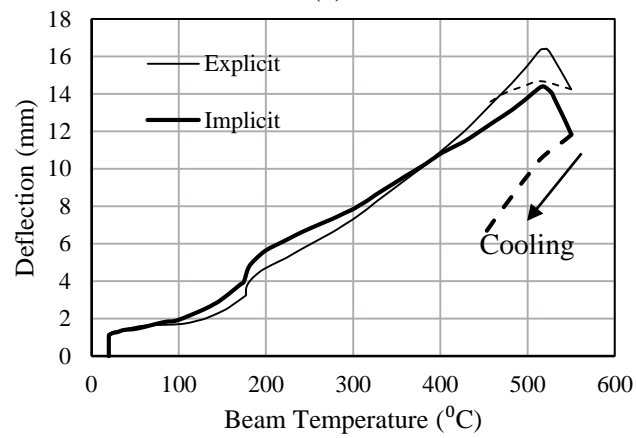


(b)

Figure. 15. Axial force and mid-span deflection for both concrete defined as plastic and using CDP: (a) axial force and (b) mid-span deflection

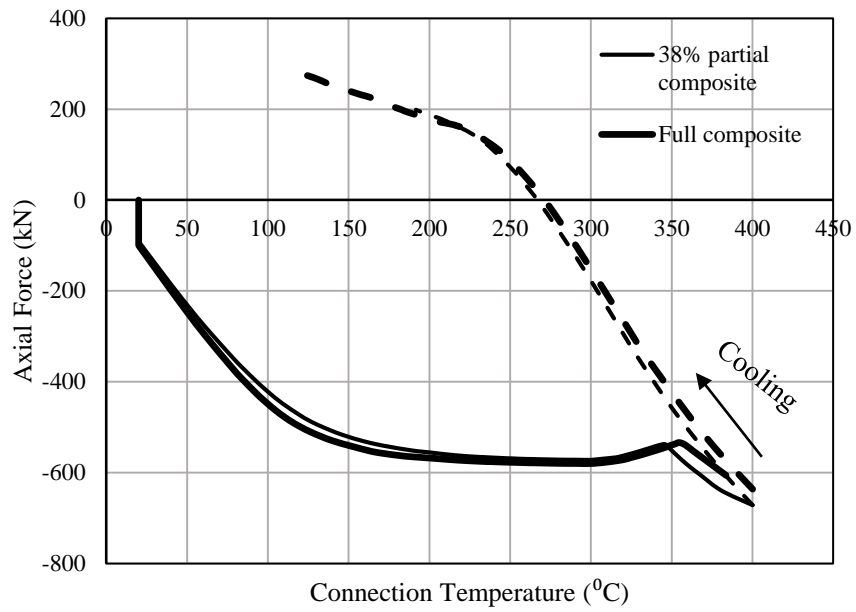


(a)

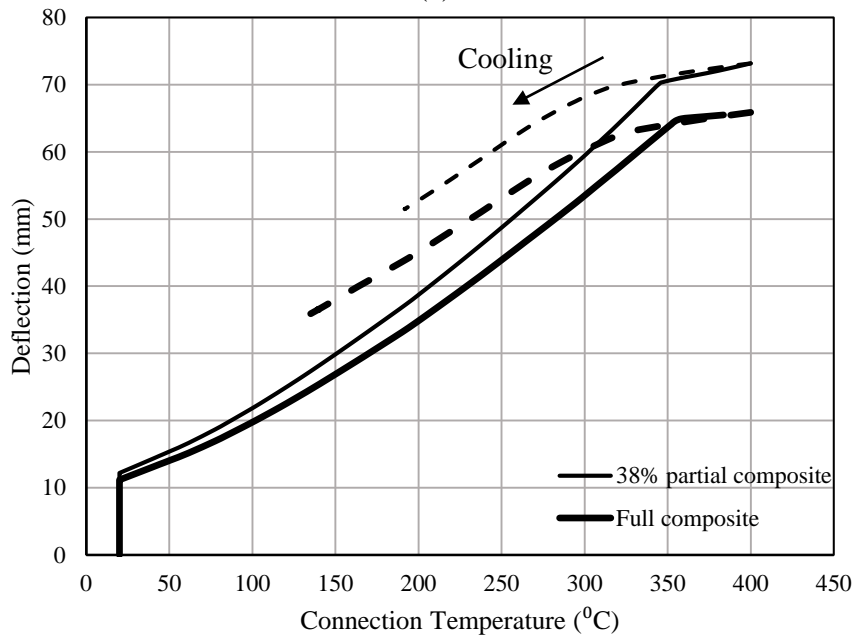


(b)

Figure. 16. Axial force and mid-span deflection using implicit and explicit concrete models: (a) axial force and (b) mid-span deflection

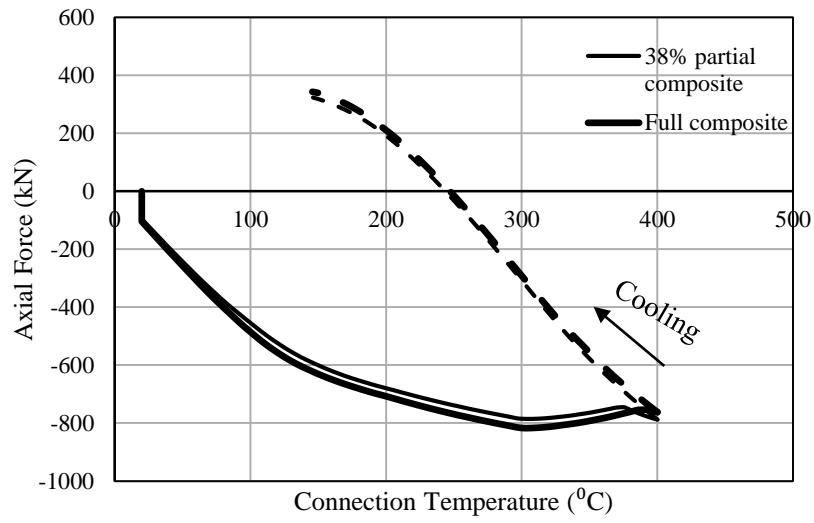


(a)

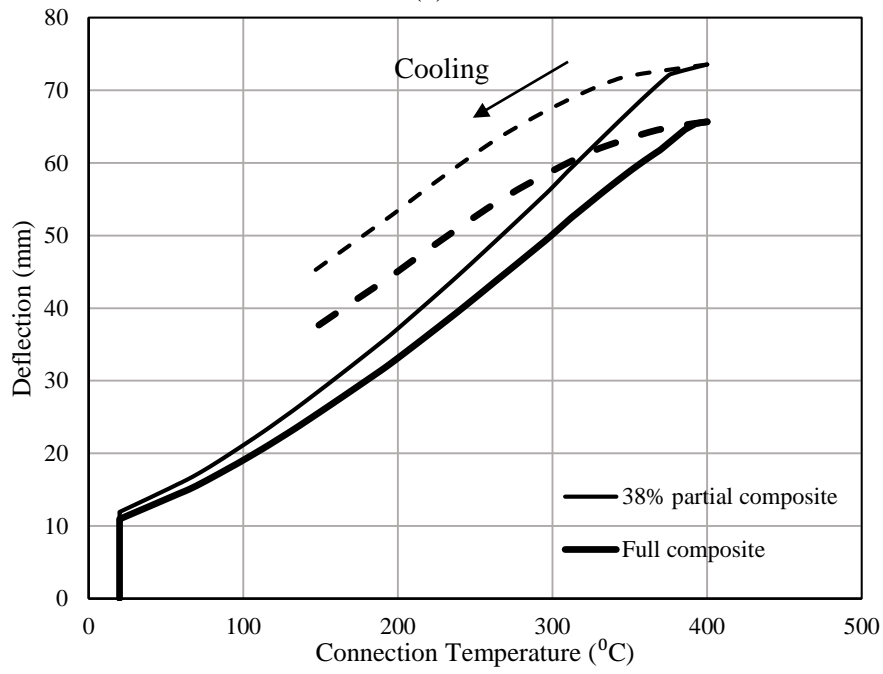


(b)

Figure. 17. Axial force and mid-span deflection for composite beams with 19 mm diameter bolts: (a) axial force and (b) mid-span deflection



(a)



(b)

Figure. 18. Axial force and mid-span deflection for composite beams with 25 mm diameter bolts: (a) axial force and (b) mid-span deflection

CHAPTER IV

RATIONAL MODEL DEVELOPMENT

During a fire event, thermal axial forces are developed in the composite beam due to the axial restraint present at the connection. The parametric study conducted in the previous section shows that significant axial forces are generated in the beam and they could lead to connection failure. For this purpose, a design oriented model is developed to predict the axial-force-temperature response of shear tab connections with composite beams when subjected to fire. The proposed rational model consists of multi-linear springs that represent the stiffness of each connection component. These multi-linear springs are combined together to predict the thermal axial response of the connection when exposed to heating-cooling cycle of a fire event. This section describes the theoretical formulation for developing the rational model and predicting the thermal axial force in the composite beam. It should be noted that the initial cooling temperature is not included in the parameters to be validated in the rational model since it did not produce a significant effect on the composite beam's response. Also, the bolt diameter and the effect of creep in the concrete are not included. Furthermore, since the load ratio in composite beams ranges between 0.45 and 0.55 (Newman et al. 2006), the rational model is developed and validated against the parameters with a load ratio of 0.5

A. Description of the behavior

Based on the FE results, a typical variation of the axial force with respect to the connection temperature is obtained and shown in Fig. 19. The behavior of the composite beam during the heating phase can be divided into four stages. The first stage (*s1*), the axial compressive force increases in the beginning of the heating phase at a constant rate.

The second stage (*s2*) starts when local buckling of the beam web occurs. In this stage, the axial compressive force continues to increase but at a slower rate. Then, yielding of the beam web occurs in the third stage (*s3*). The variation of the compressive force is largely reduced in this stage because the tangent modulus of elasticity of steel is now contributing to the axial force. Before the end of the heating phase, contact occurs between the beam bottom flange and the column flange causing the axial force to increase rapidly until the end of heating (*s4*). During the cooling phase, the composite beam contracts causing the compressive axial force to decrease. Due to cooling, the axial force becomes totally tensile around a connection temperature of 250 °C and the tensile force continues to increase until fracture of the toe of the weld occurs at a temperature of 145 °C.

B. Components Stiffnesses

The components that contribute to the overall connection stiffness are: the stiffness of the shear tab and beam web in bearing, the shear bolt stiffness, and the axial stiffness of the beam when the beam bottom flange comes in contact with the column. The components stiffnesses available in Eurocode 3 (2005) are used. The same material retention factors which are used in the FE analysis are added to the expressions obtained from Eurocode 3 (2005) to represent the stiffness of the connection at elevated temperatures.

1. Shear tab and beam web in bearing

The bearing stiffness of the shear tab/beam web, K_{br} , is computed as per Eurocode 3 (2005) and is equal to:

$$K_{br} = \frac{24n_b k_b k_t d f_u}{E} \quad (2)$$

where n_b is the number of bolt rows, k_b and k_t are factors related to the section properties as defined in Eurocode 3 part 1-8 (2005), d is the diameter of the bolt, f_u is the ultimate strength, and E is the modulus of elasticity.

2. Bolt in shear

The shear bolt stiffness, K_{bolt} , is defined as per Eurocode 3 part 1-8 (2005):

$$K_{bolt} = \frac{16n_b d^2 f_u}{E d_{M16}} \quad (3)$$

where d_{M16} is the nominal diameter of an M16 bolt type.

3. Axial stiffness of beam in contact with column

The added stiffness due to the contact between the beam bottom flange and the column, K_c , is modeled using the axial stiffness of a beam element and is equal to:

$$K_c = \frac{E_{avg.} (0.7 A_{bf})}{L} \quad (4)$$

where A_{bf} is the area of the area of the lower flange of the beam, and L is the span length, and $E_{avg.}$ is the average modulus of elasticity of steel, which will be defined in the next chapter in section 3 of the heating phase (stage 3). A reduction factor for the area equal to 0.7 is added to the formula assuming that 70% of the bottom flange area is in contact with the column flange, as observed in the FE simulations. This spring (K_c) is added to the total connection stiffness when the beam rotates enough to initiate contact between the beam and the column.

C. Equivalent Connection Stiffness

Since the number of bolts used in the shear tab connection is 4, the equivalent connection stiffness, K_e , is equal to the following:

$$K_e = 4K_{bolt-row} + K_c \quad (5)$$

K_c is added only when the contact occurs and the total stiffness of all components at each bolt, $K_{bolt-row}$, is assembled as shown in Fig. 13:

$$\frac{1}{K_{bolt-row}} = \frac{1}{k_{br,tab}} + \frac{1}{k_{bolt}} + \frac{1}{k_{br,beam}} \quad (6)$$

D. Thermal Axial Force

Having the connection stiffness, K_e , the thermal axial force, P , is determined using direct stiffness method as per Hantouche & Sleiman (2017) and it is equal to:

$$P = K_e \Delta = \frac{K_e E_s A_{bw} \alpha \Delta T}{\frac{E_s A_{bw}}{L} + K_e} \quad (7)$$

where Δ is the displacement at a given temperature, E_s is the modulus of elasticity of the steel beam, A_{bw} is the restrained area of the beam, α is the coefficient of thermal expansion, and ΔT is the temperature increment. Equation 7 is used only to get the thermal axial force developed in the steel beam. However, to take the concrete slab into consideration, the transformed concrete area, A_t , is calculated and added to A_{bw} in Eq. (7). The transformed concrete area, A_t , is equal to:

$$A_t = A_c \frac{E_c}{E_s} \quad (8)$$

where A_c is the area of the concrete slab, and E_c is the modulus of elasticity of concrete.

When the concrete strain exceeds the elastic limit, ϵ_e ($\epsilon_e = \frac{0.4f'_c}{E_c}$ (Eurocode 2 (2004))), the tangent modulus of elasticity of concrete, E_{Tc} , is used instead of the elastic modulus E_c in Eq. (8). The tangent modulus can be written as:

$$E_{T_c} = \frac{0.4f'_c}{\varepsilon_{cl} - \varepsilon_c} \quad (9)$$

where, f'_c is the concrete compressive strength, ε_c is the strain in the concrete, and ε_{cl} is the concrete strain at peak stress, defined in Eurocode 2 (2004).

Since the maximum heating temperature reached in the concrete is different than that of the beam web, Eq. (7) is modified as follows:

$$P = \frac{K_e E_s A_{bw} \alpha \Delta T_s + K_e E_s A_t \alpha \Delta T_c}{\frac{E_s A_{bw} + E_s A_t}{L} + K_e} \quad (10)$$

where A_{bw} represents the area of the beam web, ΔT_s is the temperature increment in the steel beam, and ΔT_c is the temperature increment in the concrete slab.

The analysis is performed with temperature increments of 10 °C in the steel beam. The additional thermal force at each increment is obtained and added to the force at the previous increment to obtain the total thermal axial force in the beam.

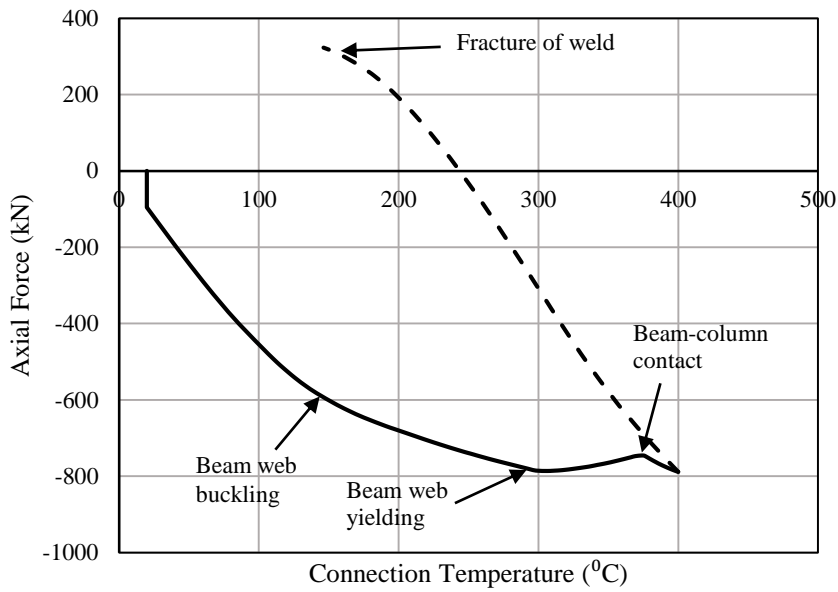


Figure. 19. Typical variation of the axial force in the composite beam with temperature

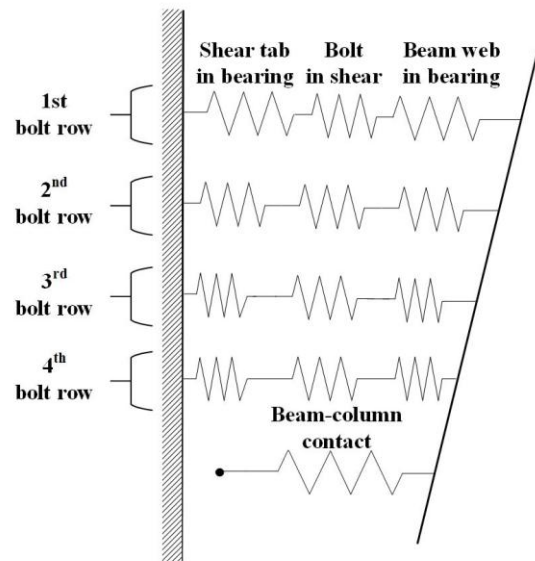


Figure. 20. Components incorporated in the assembly of the equivalent connection stiffness

CHAPTER V

FORMULATION OF THE RESPONSE FOR THE PROPOSED MODEL

A. Heating phase

The proposed model is divided into four stages during the heating phase.

1. Stage 1 (s1)

At the beginning of a fire event, thermal axial forces develop in the beam due to the restraint provided by the shear tab connection. The thermal axial force is calculated as per Eq. (10). The axial force is calculated at a temperature increment of 10 °C and then added to the previous increments to obtain the total axial force at each temperature. The axial force continues to increase at the same rate until beam web local buckling occurs. Buckling of the beam web occurs when the axial force exceeds the critical web buckling force, P_{cr} , which is determined according as per Selamet & Garlock (2013).

2. Stage 2 (s2)

When local buckling of the beam web occurs, only half the area of the beam web is considered in computing the axial force (Rhodes (2003)). The compressive axial force can then be written as follows:

$$P = \frac{K_e E_s 0.5 A_{bw} \alpha \Delta T_s + K_e E_s A_t \alpha \Delta T_c}{\frac{E_s 0.5 A_{bw} + E_s A_t}{L} + K_e} \quad (11)$$

The axial force keeps increasing in this stage but at a slower rate than the previous one until yielding of the beam web occurs. Yielding of the beam web occurs when the compressive axial force reaches the critical yielding force, P_y :

$$P_y = A_{bw} f_y \quad (12)$$

where f_y is the yield strength of the steel beam.

3. Stage 3 (s3)

Beam web yielding occurs at the early stages of heating. The yielding progresses with temperature until the total area of the web yields when the axial force reaches P_y . The ratio of the yielded area of the beam web, A_{by} , (from FE results) to the total beam web area is plotted against temperature as shown in Fig. 21. It can be seen that the ratio of the area follows a linear relation with respect to temperature. Therefore, the yielded area of the beam web, A_{by} , at any given temperature can be written as a linear relationships follows:

$$\frac{A_{by}}{A_{bw}} = aT + b \quad (13)$$

where a and b are constants derived from the FE results.

In this case, the modulus elasticity of the beam web is taken as an average between the yielded and non-yielded portions of the web. The steel elastic modulus $E_{avg.}$ to be used to determine the thermal axial force is:

$$E_{avg.} = \frac{E_s (A_{bw} - A_{by}) + E_{Ts} A_{by}}{A_{bw}} \quad (14)$$

where E_{Ts} is the tangent modulus of steel.

The thermal axial force can be written as:

$$P = \frac{K_e E_{avg.} 0.5 A_{bw} \alpha \Delta T_s + K_e E_s A_t \alpha \Delta T_c}{\frac{E_{avg.} 0.5 A_{bw} + E_s A_t}{L} + K_e} \quad (15)$$

In this stage the axial force continues to increase with a slow rate. This is due to the reduction in the modulus of elasticity. This process continues until contact between

the beam bottom flange and the column flange occurs. Contact is determined by checking the beam end rotation at each temperature increment. The rotation at which the contact occurs, θ_c , is found equal to:

$$\theta_c = \frac{s}{h/2} \quad (16)$$

where s is the setback distance and h is the steel beam height.

Since the composite beam with shear tab connection is considered as a simply supported beam. The beam end rotation, θ , can be calculated as per Selamet & Garlock (2012) as follows:

$$\theta = \frac{wL^3}{E_s I} \quad (17)$$

where w is the applied load on the beam and I is the moment of inertia the composite beam. The moment of inertia of the composite beam, I , is computed after obtaining the transformed concrete area as per Eq. (8). The rotation, θ , increases with temperature due to the reduction in the modulus of elasticity and the moment of inertia until it reaches θ_c where contact is likely to occur.

4. Stage 4 (s4)

After contact occurs, the equivalent stiffness of the connection K_e increases. This is manifested in the model by adding the contact stiffness K_c to the expression of the equivalent stiffness K_e as per Eq. (6). In addition, the area of the beam contributing to the axial force increases since the bottom flange is now considered restrained. Eq. (8) becomes as:

$$P = \frac{K_e E_{avg.} (0.5A_{bw} + 0.7A_{bf}) \alpha \Delta T_s + K_e E_s A_t \alpha \Delta T_c}{\frac{E_{avg.} 0.5A_{bw} + E_s A_t}{L} + K_e} \quad (18)$$

The thermal compressive force increases in this stage at a faster rate than the previous stage due to contact. The force continues to increase until the end of the heating phase unless any failure occurs.

B. Cooling phase

The cooling phase is composed of four stages.

5. Stage 5 (s5)

The main difference between this stage and the previous one is that the elastic modulus of steel, E_s , is used in the calculations to obtain the numerator of Eq. (18) instead of $E_{avg.}$. This is because the numerator of Eq. (18) corresponds to the thermal restraint axial force which is related to the recovered elastic strain during unloading. The temperature increment to be used in this case is equal to -10 °C. The change in the thermal axial force is calculated as follows:

$$P = \frac{K_e E_s (0.5A_{bw} + 0.7A_{bf}) \alpha \Delta T_s + K_e E_s A_t \alpha \Delta T_c}{\frac{E_{avg.} 0.5A_{bw} + E_s A_t}{L} + K_e} \quad (19)$$

The compressive axial force keeps decreasing until there is no contact between the beam flange and the column flange. The beam rotation, calculated according to Eq. (17), decreases with temperature due to the recovery of the material properties. This stage ends when the rotation becomes less than the contact rotation θ_c .

6. Stage 6 (s6)

The contact stiffness K_c is subtracted from the equivalent connection stiffness. Also, the bottom flange area does not contribute anymore to the axial force. Therefore, the thermal axial force can be written as:

$$P = \frac{K_e E_s 0.5 A_{bw} \alpha \Delta T_s + K_e E_s A_t \alpha \Delta T_c}{\frac{E_{avg.} 0.5 A_{bw} + E_s A_t}{L} + K_e} \quad (20)$$

The axial force decreases in this stage at a lower rate than the previous stage. This state continues until the compressive force becomes less than the critical buckling force, P_{cr} , as calculated according to Selamet & Garlock (2013).

7. Stage 7 (s7)

After the axial force becomes lower than P_{cr} , it is assumed that the buckled area of the web is recovered and the total area of the web now contributes to the thermal force. This is observed in the FE results where the beam web regains its original shape during the cooling phase. The thermal axial force can be written as:

$$P = \frac{K_e E_s A_{bw} \alpha \Delta T_s + K_e E_s A_t \alpha \Delta T_c}{\frac{E_{avg.} A_{bw} + E_s A_t}{L} + K_e} \quad (21)$$

The compressive force continues to decrease until it turns into tensile force.

8. Stage 8 (s8)

When the axial force becomes tensile, the concrete is considered as cracked and is not included in the model. The steel beam web is the only component contributing to the axial force. The term for the thermal axial force can be written as:

$$P = \frac{K_e E_s A_{bw} \alpha \Delta T_s}{\frac{E_{avg.} A_{bw}}{L} + K_e} \quad (22)$$

The tensile force increases in this stage at the same rate until failure occurs by fracture of the weld.

A typical variation of the beam axial force with temperature is shown in Fig. 22, along with a summary of the all the stages that characterize the behavior of the composite beam during heating and cooling phases of the fire.

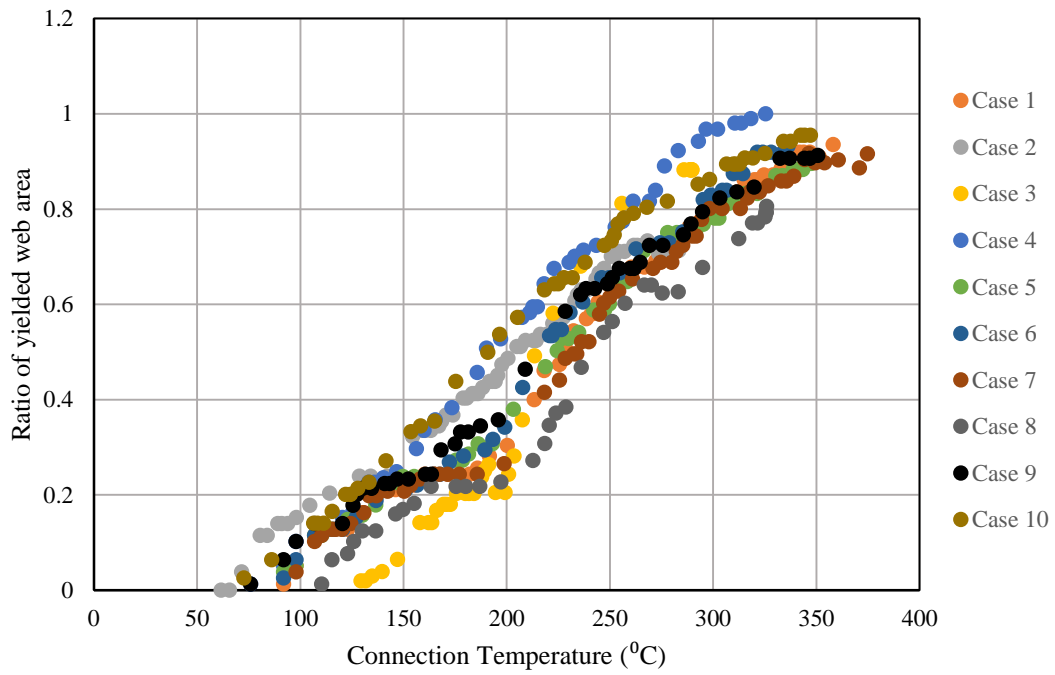


Figure. 21. Ratio of the yielded area of the beam web to the total web area (A_{by} / A_{bw}) against temperature

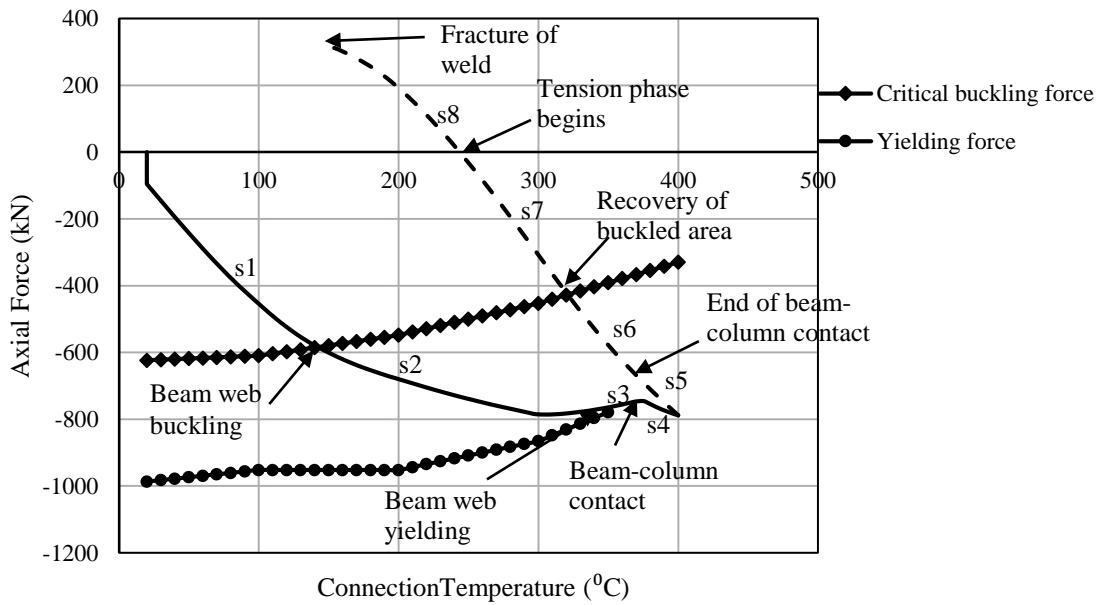


Figure. 22. Summary of different stages present in the proposed model

CHAPTER VI

PROPOSED MODEL PERFORMANCE

The proposed rational model is compared to the FE results obtained from the parametric study. Figures 23 and 24 show a comparison of the rational model with the FE results for all cases (see Table 1). It can be seen that the proposed model predicts with good accuracy the axial force developed in the composite beam when under transient fire conditions for all cases. Therefore, the proposed model can be used as a tool to develop design guidelines for shear tab connections with composite beams subjected to fire temperatures having different geometric and material properties.

Table 1. Parametric study cases in FE modeling

Case	Column section	Beam section	Beam length m (ft.)	Shear tab thickness mm (in.)	Shear tab location mm (in.)	Slab thickness mm (in.)	Setback distance mm (in.)	Percentage of composite action
1	W 14x90	W 16x36	6.10 (20)	9.5 (0.375)	0	91 (3.6)	20 (0.8)	100
2	W 14x90	W 16x36	9.15 (30)	9.5 (0.375)	0	91 (3.6)	20 (0.8)	100
3	W 14x90	W 16x36	12.20	9.5 (0.375)	0	91 (3.6)	20 (0.8)	100
4	W 14x90	W 16x36	6.10 (20)	12.7 mm (0.5)	0	91 (3.6)	20 (0.8)	100
5	W 14x90	W 16x36	6.10 (20)	9.5 (0.375)	20 (0.8)	91 (3.6)	20 (0.8)	100
6	W 14x90	W 16x36	6.10 (20)	9.5 (0.375)	0	66 (2.6)	20 (0.8)	100
7	W 14x90	W 16x36	6.10 (20)	9.5 (0.375)	0	114 (4.5)	20 (0.8)	100
8	W 14x90	W 16x36	6.10 (20)	9.5 (0.375)	0	91 (3.6)	12.7 (0.5)	100
9	W 14x90	W 16x36	6.10 (20)	9.5 (0.375)	0	91 (3.6)	25.4 (1)	100
10	W 14x90	W 16x36	6.10 (20)	9.5 (0.375)	0	91 (3.6)	20 (0.8)	37

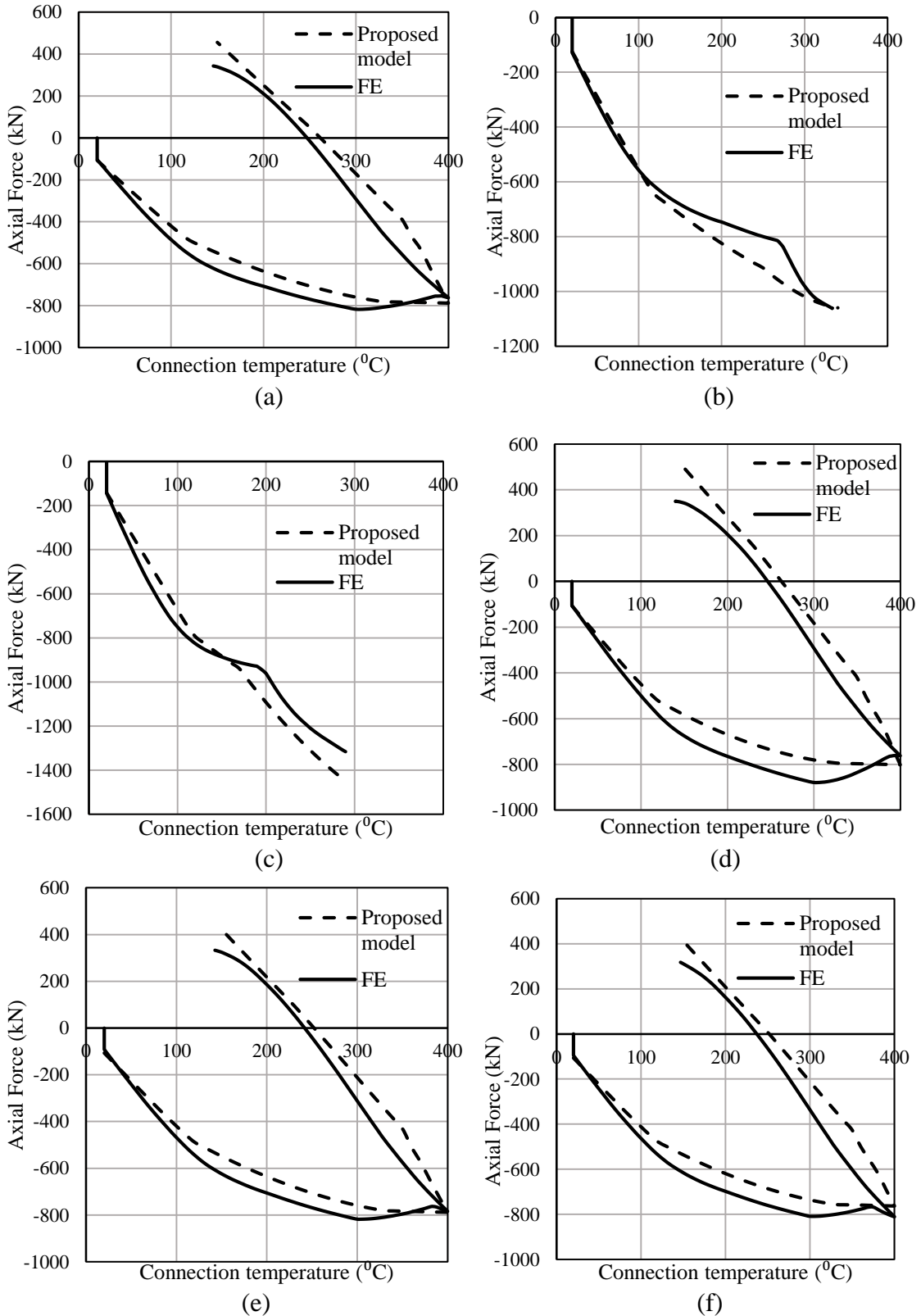
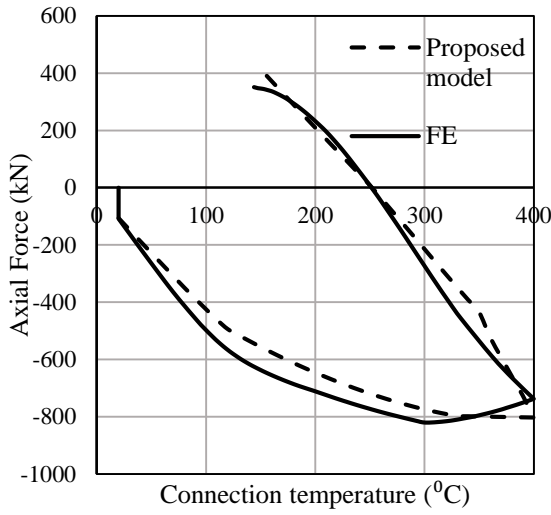
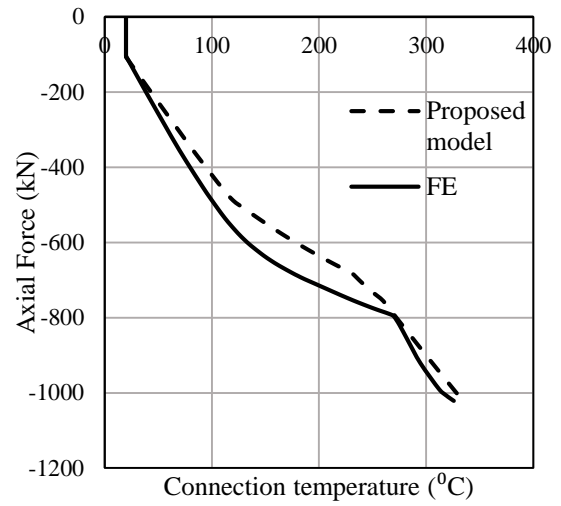


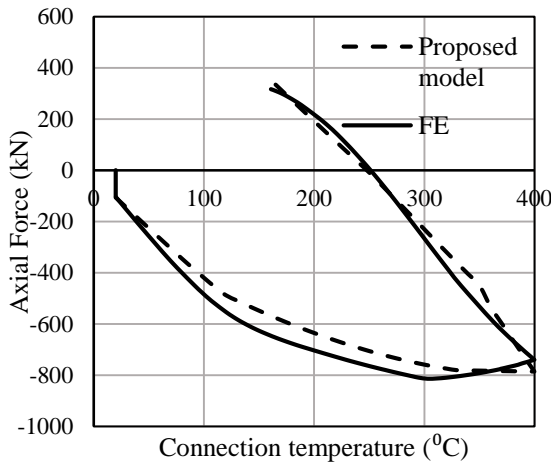
Figure. 23. Proposed model vs. FE results (a) Case 1, (b) Case 2, (c) Case 3, (d) Case 4, (e) Case 5, (f) Case 6



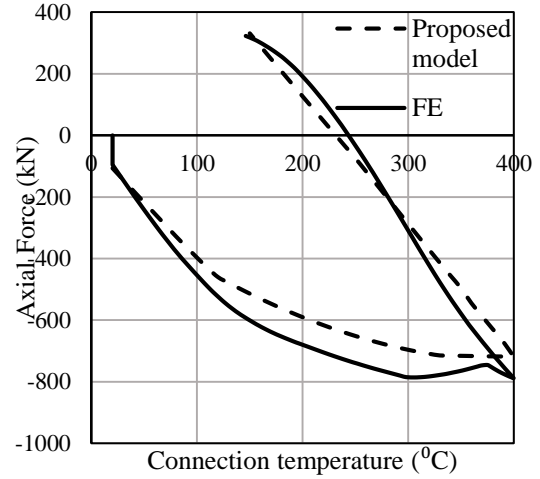
(a)



(b)



(c)



(d)

Figure. 24. Proposed model vs. FE results (a) Case 7, (b) Case 8, (c) Case 9, (d) Case 10

CHAPTER VI

SUMMARY, CONCLUSIONS AND RECOMMENDATIONS

A. Summary and Conclusions

This research presents an investigation of the behavior of shear tab connections with composite beams when subjected to fire temperatures, using FE and rational models. To achieve this goal, FE models of shear tab connections with composite beams are developed in ABAQUS and validated against experimental data conducted by Selden et al. (2014). Heat transfer analysis is performed to predict the temperature distribution in the composite beam. A series of FE simulations are then performed to identify the key parameters that affect their behavior under fire. Gravity loads are applied first to the composite beam studied. Then, the beam is heated to the desired temperature and cooled back to ambient temperature, while keeping the applied load constant. The parameters varied include the geometrical components of both the composite beam and the connection, degree of composite action and creep effect in the concrete. The FE analysis shows that large thermal axial forces are developed in the composite beam during a fire event, leading to failure of the connection. Based on the FE results, a rational model is developed to predict the axial force-temperature response of shear tab connections with composite beams in fire. The proposed model is formed of different springs that represent the stiffness of each component in the connection, the steel beam, the concrete slab and the degree of composite action as well. However, the effect of creep in the concrete is not included in this model.

The following points are concluded from this study:

- The FE model is able to predict the deflection and the load deformation-response when compared with experimental results. Also, both FE and the experimental results show that shear tab connection survived the heating phase and fracture at the toe of the weld occurred in the cooling phase. It should be noted that fracture modeling is not included in the simulations.
- The parametric study performed shows that large axial forces develop at high temperatures in the connection. The thermal forces are compressive in the heating phase and they turn into tensile in the cooling phase.
- The results show that as the beam undergoes a large deflection, contact initiates between the beam's bottom flange and the column flange (starting from a connection temperature of 250 °C) causing an increase in the axial force. The increase in the axial force could reach 400 kN and might lead to failure. Increasing the slab temperature, the slab thickness, or the bolt diameter reduces the deflection and consequently avoids the contact between the beam and the column.
- Thermal creep in the concrete has a major effect on the deflection response of the composite beam. Including the creep effect in the concrete affects the deflection response for temperatures above 250 °C. Larger deflections occur during the cooling phase due to the unrecovered creep strain. The large deflections can cause contact to occur between the beam and the column, resulting in larger axial forces. Note that the effect of creep in the steel is not included in the analysis.
- Partial composite action induces larger deflection, but it has no significant impact on the forces in the beam nor on the failure mode.
- Most of the parametric analysis indicates that the shear tab connection survived the heating phase and failed in the cooling phase at the toe of the weld. During the cooling

phase, the applied load gradually changes from flexural to tensile until the tensile axial force exceeds the tensile capacity of the weld leading to fracture at the toe of the weld.

- A characterization of the force-temperature response is provided. The behavior can be divided into eight stages. A rational model is developed accordingly to predict the variation of the thermal axial force in the composite beam with respect to the connection temperature. The rational model includes the stiffness of each component in the connection, the steel beam stiffness, and the concrete slab stiffness as well.
- The rational model predicts with good accuracy the thermal induced axial forces in the beam during a fire event. The results obtained from the rational model are in good agreement with the FE results. It should be noted that the effect of creep is not included in the analysis.
- The rational model can be used as a reliable tool to predict the thermal axial force demands in shear tab connections with composite beams. The main advantage of this model is that it requires much less computational effort than that required by FE analysis. Also, the proposed model can be used in performance-based approaches in future structural fire engineering applications.

B. Recommendations

This research provides an insight on the response of composite beams under fire and the generated thermal axial forces. However, more research work still needs to be conducted in order to develop a full understanding of the behavior of composite beams with simple connections subjected to fire. Additional studies that help achieve this objective are the following:

- Fracture modeling needs to be adopted in all FE models which allows a post-yielding analysis of the connection response under fire.
- Further experimental works need to be conducted with composite beams of different steel connections.
- Additional experiments are needed to obtain more reliable material properties of steel and concrete at elevated temperatures.
- More FE simulations are required to better examine the thermal effect of creep in the steel and in the concrete, including the cases where the PNA is in the concrete slab and part of the concrete is subjected to tension.
- Improving the accuracy of the proposed model by taking the effect of creep in both steel and concrete into consideration.
- More FE simulations are needed to include geometric parameters such as number of bolts and the bolt diameter in order to extend the applicability of the proposed model.

BIBLOGHRAPHY

- Agarwal, A., Selden, K. & Varma, A. (2014). "Stability behavior of steel building structures in fire conditions: Role of Composite Floor System with Shear-Tab Connections". *Journal of Structural Fire Engineering*, 5(2), 77-96.
- Choe, L., Ramesh, S., Hoehler, M., & Gross, J. (2018). Experimental Study on Long-Span Composite Floor Beams Subject to Fire: Baseline Data at Ambient Temperature. *Structures Congress 2018*.
- Code clinic: For study of AWS D1.1/D1. 1M: 2010 structural welding code -- steel*. (2010). Miami, FL: American Welding Society.
- Eurocode 2: Design of concrete structures - part 1-2: General rules - structural fire design*. (1995). Brussels: European Committee for Standardization.
- Eurocode 2: Design of concrete structures - part 1-2: General rules - structural fire design*. (2004). Brussels: European Committee for Standardization.
- Eurocode 3: Design of steel structures - part 1-2: General rules - structural fire design*. (2005). Brussels: European Committee for Standardization.
- Eurocode 3: Design of steel structures - part 1-8: Design of joints*. (2005). Brussels: European Committee for Standardization.
- Eurocode 4: Design of composite steel and concrete structures - part 1-2: General rules - structural fire design*. (2005). Brussels: European Committee for Standardization.
- El Ghor, A. H., & Hantouche, E. G. (2017). "Thermal creep mechanical-based modeling for flush endplate connections in fire". *Journal of Constructional Steel Research*, 136, 11-23.
- Final report on the collapse of the World Trade Center towers*. (2005). Gaithersburg, MD: U.S. Dept. of Commerce, Technology Administration, National Institute of Standards and Technology.
- Fischer, E.C. & Varma, A.H. (2015). "Fire behavior of composite beams with simple connections: Benchmarking of numerical models". *Journal of Constructional Steel Research*, 111, 112-125.
- Fischer, E.C. & Varma, A.H. (2017). "Fire resilience of composite beams with simple connections: Parametric studies and design". *Journal of Constructional Steel Research*, 128, 119-135.
- Garlock, M.E. & Selamet, S. (2010). "Modeling and behavior of steel plate connections subject to various fire scenarios". *Journal of Structural Engineering*, 136(7), 897-906.

- Gernay, T. & Franssen, J.-M. (2012). "A formulation of the Eurocode 2 concrete model at elevated temperature that includes an explicit term for transient creep". *Fire Safety Journal*, 51, 1-9.
- Hantouche, E.G. & Sleiman, S.A. (2017). "Axial restraint forces in shear endplates of steel frames due to fire". *Journal of Constructional Steel Research*, 128, 528-541.
- Hantouche, E.G., Jabotian, H.V., Al Khatib, K.A., El Ghor, A.H. & Morovat, M.A. (2018), A Unified Mechanical Model for Fire Design of Simple Steel Connections. *Structures Congress 2018*.
- Hu, G., Morovat, M.A., Lee, J., Schell, E. & Engelhardt, M.D. (2009). "Elevated temperature properties of ASTM A992 steel". *Structures Congress 2009*, 1067-1076.
- Hu, Y., Davison, B., Burgess, I., & Plank, R. (2009). "Component modelling of flexible end-plate connections in fire". *International Journal of Steel Structures*, 9(1), 1-15.
- Jones, L. C. (1997). *The influence of semi-rigid connections on the performance of steel framed structures in fire*. University of Sheffield.
- Koduru, S. D., & Driver, R. G. (2014). "Generalized Component-Based Model for Shear Tab Connections". *Journal of Structural Engineering*, 140(2), 04013041.
- Lee, J. & Fenves, G.L. (1998), "Plastic-damage model for cyclic loading of concrete structures", *Journal of Engineering Mechanics*, 124(8), 892-900.
- Minimum design loads and associated criteria for buildings and other structures*. (2017). Reston, VA: American Society of Civil Engineers (ASCE).
- Newman, G. M., Robinson, J. T., & Bailey, C. G. (2006). *Fire safe design: A new approach to multi-storey steel-framed buildings*. Ascot: The Steel Construction Institute.
- Pakala, P. & Kodur, V. (2016). "Effect of concrete slab on the behavior of fire exposed subframe assemblies with bolted double angle connections". *Engineering Structures*, 107, 101-115.
- Phan, L.T., McAllister, T.P., Gross, J.L. & Hurley, M.J. (2010), *Best Practice Guidelines for Structural Fire Resistance Design of Concrete and Steel Buildings*, National Institute of Standards and Technology (NIST), Gaithersburg, MD.
- Piluso, V., Rizzano, G., & Tolone, I. (2012). "An advanced mechanical model for composite connections under hogging/sagging moments". *Journal of Constructional Steel Research*, 72, 35-50.
- Rhodes, J. (2001). "Some observations on the post-buckling behaviour of thin plates and thin-walled members". *Thin-Walled Structures - Advances and Developments*, 41, 69-84.

- Sarraj, M. (2007). *The behaviour of steel fin plate connections in fire*. Sheffield: University of Sheffield.
- Selamet, S. & Garlock, M.E. (2012). "Predicting the maximum compressive beam axial force during fire considering local buckling". *Journal of Constructional Steel Research*, 71, 189-201.
- Selamet, S. & Garlock, M.E. (2013). "Plate Buckling Strength of Steel Wide-Flange Sections at Elevated Temperatures". *Journal of Structural Engineering*, 139(11), 1853-1865.
- Selamet, S. & Bolukbas, C. (2016). "Fire resilience of shear connections in a composite floor: Numerical investigation". *Fire Safety Journal*, 81, 97-108.
- Selden, K.L., Fischer, E.C. & Varma, A.H. (2014). "Advanced fire testing of a composite beam with shear tab connections". *Structures Congress 2014*, 1170-1174.
- Selden, K.L., Fischer, E.C. & Varma, A.H. (2016). "Experimental investigation of composite beams with shear connections subjected to fire loading". *Journal of Structural Engineering*, 142(2), 1-12.
- Selden, K.L. & Varma, A.H. (2016), "Composite beams under fire loading: numerical modeling of behavior", *Journal of Structural Fire Engineering*, 7(2), 142-157.
- Steel construction manual*. (2010). Chicago, IL: American Institute of Steel Construction (AISC).
- Steel construction manual*. (2016). Chicago, IL: American Institute of Steel Construction (AISC).
- Tarantino, A.M. & Dezi, L. (1992), "Creep effects in composite beams with flexible shear connectors", *Journal of Structural Engineering*, 118(8), 2063-2080.
- Wald, F., Simões da Silva, L., Moore, D.B, Lennon, T., Chladna, M., Santiago, A., Benes, M. & Borges, L.A. (2006), "Experimental behaviour of a steel structure under natural fire", *Fire Safety Journal*, 41(7), 509-522.
- Wang, W., Huang, G.-S., Li, G.-Q. & Engelhardt, M.D. (2016), "Behavior of steel-concrete partially composite beams subjected to fire-Part 1: Experimental study", *Fire Technology*, 53(3), 1039-1058.
- Wang, W., Wang, K., Li, G. & Engelhardt, M.D. (2016), "Behavior of steel-concrete partially composite beams subjected to fire-Part 2: Analytical study", *Fire Technology*, 53(3), 1147-1170.
- Zhao, B., & Kruppa, J. (1997). *Fire resistance of composite slabs with profiled steel sheet and of composite steel concrete beams: Final report*. European Commission.